NASA TN D-1493

c.1

TECHNICAL NOTE

D-1493

ENVIRONMENTAL PROBLEMS OF SPACE FLIGHT STRUCTURES

II. METEOROID HAZARD

Prepared by John R. Davidson and Paul E. Sandorff in collaboration with the
NASA Research Advisory Committee on Missile
and Space Vehicle Structures

Langley Research Center
Langley Station, Hampton, Va.

NATIONAL AERONAUTICS AND SPACE ADMINISTRATION

WASHINGTON

January 1963

TABLE OF CONTENTS

	Page
PREFACE	ii
MEMBERS OF THE NASA RESEARCH ADVISORY COMMITTEE ON MISSILE AND SPACE VEHICLE STRUCTURES	iii
SUMMARY	1
INTRODUCTION	1
SYMBOLS	2
METEOROID ENVIRONMENT	4
Asteroidal Particles	4
Cometary Particles	5
Tektites	8
Pertubation Forces	9
Observations of Meteors From the Earth	10
Satellites and Space Probes	15
Research in Progress	18
INTERACTION BETWEEN METEOROID ENVIRONMENT AND STRUCTURE	19
Historical Aspects of the Plate Perforation Problem	19
Physical Description of High-Speed Impact Phenomena	20
Modern Theories of Penetration	22
Experimental Data	26
PROTECTION METHODS	30
Types of Structural Damage	30
Application of Meteoroid Flux Data and Impact Data to Design Problems	30
RESEARCH IN PROGRESS	36
Ground Research	36
Flight Test Research	36
RECOMMENDED METEOROID RESEARCH PROGRAM	36
REFERENCES	40
BIBLIOGRAPHY	47
TABLES	49
FIGURES	61

PREFACE

The exploration, study, and definition of the environmental conditions which exist in space beyond the earth's atmosphere form an essential part of the current space-age effort. The development of this science is of especial interest to the vehicle structures designer, who must make decisions today that will establish the capability and efficiency of the space hardware in use 5 or 10 years hence. The time, the tools, and the money available for obtaining necessary engineering data concerning space environment are limited. It is therefore of utmost importance that the total national effort be coordinated and directed to bring maximum returns.

Recognizing the urgency of this situation, the NASA Research Advisory Committee on Missile and Space Vehicle Structures has appointed an Environmental Task Force to review the problems and recommend appropriate action. The result will be a series of definitive reports, each dealing with an important space-age design environmental problem, which are intended to present not only the present state of knowledge but to indicate what is being done on a national scale, and to make recommendations regarding the direction of future effort. These reports will be prepared primarily by NASA technical personnel but with the critical assistance of the entire committee. The subject of the present study is the problem of the meteoroid environment for cislunar vehicles.

E. E. Sechler, Chairman
NASA Research Advisory Committee on
Missile and Space Vehicle Structures

MEMBERS OF THE NASA RESEARCH ADVISORY COMMITTEE ON

MISSILE AND SPACE VEHICLE STRUCTURES

Professor E. E. Sechler, Chairman
California Institute of Technology

Mr. Lewis H. Abraham
Douglas Aircraft Company, Inc.

Mr. Marshall E. Alper
Jet Propulsion Laboratory

Dr. Millard V. Barton
Space Technology Laboratories, Inc.

Mr. G. B. Butters
Department of the Navy

Mr. Edwin G. Czarnecki
The Boeing Company

Mr. Norris F. Dow
General Electric Company

Mr. Albert L. Erickson
NASA Ames Research Center

Mr. Jack B. Esgar
NASA Lewis Research Center

Major Earl R. Gieseman, Jr.
U.S. Air Force

Major Truman L. Griswold
U.S. Air Force

Mr. H. A. Heithecker
Army Ballistic Missile Agency

Mr. Norman J. Mayer, Secretary
NASA Headquarters

Mr. Richard R. Heldenfels
NASA Langley Research Center

Mr. Emil A. Hellebrand
NASA George C. Marshall Space
Flight Center

Mr. A. J. Kullas
Martin-Marietta Corporation

Mr. William R. Micks
The RAND Corporation

Mr. S. Joseph Pipitone
Goodyear Aircraft Corporation

Mr. Louis A. Riedinger
Lockheed Missiles and Space Company

Professor Paul E. Sandorff
Lockheed Missiles and Space Company

Dr. Hans U. Schuerch
Astro Research Corporation

Mr. Robert S. Shorey
General Dynamics Corporation

Mr. Robert E. Vale
NASA Manned Spacecraft Center

NATIONAL AERONAUTICS AND SPACE ADMINISTRATION

TECHNICAL NOTE D-1493

ENVIRONMENTAL PROBLEMS OF SPACE FLIGHT STRUCTURES

II. METEOROID HAZARD*

Prepared by John R. Davidson and Paul E. Sandorff in collaboration with the
NASA Research Advisory Committee on Missile
and Space Vehicle Structures

SUMMARY

The meteoroid environment and the effects of hypervelocity impact on space vehicles are described, and the effects of the incompleteness of present knowledge of each are discussed. The overall problem of the meteoroid hazard is evaluated and methods of eliminating the probability of meteoroid damage are given. A partial listing of typical research projects on meteoroid-environment and hypervelocity-impact problems is presented.

INTRODUCTION

Space environment - the conditions that exist beyond the atmosphere, their exploration, study, and ultimate incorporation into the known world of science - is a fascinating and well-supported part of current space-age effort. To the structures designer, however, it often appears as though many aspects which would immediately affect the efficiency and the integrity of design are being overlooked and that research objectives do not follow an optimum plan. Frequently experiments are purely scientific, being directed at knowledge for the sake of knowledge; often they are severely pragmatic, but with respect to applications which are as yet many years in the future. Meanwhile, the pursuit of immediately useful engineering data, which could be applied to effect immediate advances in the overall performance of the vehicles being designed today, is being accorded secondary importance.

Space vehicles must incorporate some provision for thwarting damage from meteoroid encounters. The "shirt-sleeve" environment envisioned for journeys which have periods of a week or more precludes permitting the walls of the pressurized cabin to be punctured. Propellant tanks must not be punctured, and heat-shield surfaces cannot be deeply pitted if they are to perform satisfactorily during atmospheric entry. Spalling from internal surfaces due to impact may have serious consequences on men and equipment, even though complete puncture does not occur.

---

*Part I is NASA Technical Note D-1474 by Louis F. Vosteen.

The recent interest in space journeys is accompanied by some apprehension about the danger presented by meteoroids to vehicles which are not provided with the protection of the Earth's atmosphere. An early examination of the meteoroid hazard was made by Grimminger (ref. 1). In order to estimate the severity of this hazard, the known data and hypotheses associated with meteoritic particles are reviewed herein. An hypothesis explaining the origin of meteoroids and meteors is presented by F. L. Whipple of Harvard University (see refs. 2 to 7). This hypothesis is generally compatible with the few known facts and with data obtained during the last 5 years.

The results of collisions between meteoroids and space vehicles are dependent upon the penetration effects of high-speed particles on engineering materials. Great efforts have been made to ascertain a workable method of predicting the effects of high-speed impacts. Some results of these efforts are reviewed herein.

Throughout the present paper the word "meteoroid" is used as a general term to refer to particles traveling in space. The word "meteor" is used to denote the luminous phenomena exhibited by particles as they enter our atmosphere at high speeds. "Meteorite" will be reserved to designate an extraterrestrial body found on the Earth's surface.

Several summary reports which pertain to various segments of the meteoroid problem are available. References 8 and 9 contain summaries of the data on dust particles gathered by satellites and rocket probes. Reference 10 is a summary and compilation of data from ground-based facility tests on hypervelocity impact. Reference 11 is a summary of the meteoroid hazard and contains an analysis of experiment requirements for flight-test evaluation of this hazard. In addition to the numbered references, this paper contains a bibliography of related material.

SYMBOLS

A	area, m^2 or ft^2
b	minimum momentum per unit area to effect penetration, $kg\text{-}m^{-1}\text{-}sec^{-1}$
c	longitudinal bar sonic velocity, m/sec
$\bar{c}$	dilatational bulk sonic velocity, m/sec
d	diameter, m
E	modulus of elasticity, newton-m^2 (1 newton = 10^5 dynes)
H	Brinell hardness number
h	spacing between sheets, in.
K	constant
l	length, m

M	visual magnitude
m	mass, kg
N	number
n	index number
P	depth of penetration, m
$\bar{P}$	depth of penetration; not specified whether from original surface to crater bottom, or original surface to top of deposited material in crater, m
p	probability
R	radius, m
r	number
T	kinetic energy, joule
t	thickness, m, cm, or in., as used
u	velocity of plastic wave propagation in material, m/sec
V	velocity, m/sec
V_L	limiting velocity
V_o	minimum velocity required to effect penetration, m/sec
v	volume, m^3
α	constant
β	luminous efficiency
ϵ	most probable number
ζ	heat required to melt target material (from initial temperature of material), joule/kg
μ	Poisson's ratio
ξ	constant
ρ	density, kg/m^3
σ_y	yield stress, $newton/m^2$

τ time, sec

ψ penetration flux, holes-ft^{-2}-day^{-1}

Subscripts:

b total thickness of bumper and main wall

c crater

p projectile

t target

0 zero on visual magnitude scale

1,2 integers

METEOROID ENVIRONMENT

At present, it is believed that meteoroids may be divided into two groups defined by their origin: (1) meteoroids from asteroids, and (2) meteoroids from comets. Each of these groups will be discussed separately.

Asteroidal Particles

The asteroidal particles constitute less than 10 percent of the total influx of the particles which enter the Earth's atmosphere. It is believed that these particles originate in the asteroidal belt which is located between the orbits of Mars and Jupiter. A present theory is that the asteroids are the remains of one or more planets which had orbits located somewhere between the orbits of Mars and Jupiter. The asteroids are irregularly shaped rocky bodies; the largest one is about 500 miles in its longest dimension, and the smallest observable ones are on the order of 1 mile or less. The asteroids are noted for their highly elliptic orbits. Various perturbation forces influence the orbits of the asteroidal particles in such a way that small particles from them occasionally cross the path of the Earth. Some of these enter the Earth's atmosphere and become meteors.

The large size and physical solidity of some of the meteorites have enabled them to survive the severe aerodynamic heating experienced during entry into the Earth's atmosphere at extremely high speeds. The meteorite protects itself by ablating a portion of its outside surface; the flow lines of molten material can be seen in the cross sections of many meteorites. The cross sections show a residual layer of oxide on the outside surface which is on the order of a few thousandths of an inch deep. The main-body chemical composition is iron, nickel, and stone; some meteorites are mostly iron and others mostly stone, but a large proportion are a combination of all three. Many meteorites resemble terrestrial

rocks, but the meteoritic mineral forms are different from earth stones. It is hoped that close physical and chemical scrutiny of meteorites may provide information about their origin and the conditions under which they were originally formed.

The sizes of the meteorites found on the ground range from many tons to particles only a few microns in diameter. Extremely small meteorites have been trapped on sticky surfaces located on rooftops, towers, mountain tops, and high-flying aircraft. As the size of the particles decreases, the number increases. Fortunately only a few of the extremely large particles strike the Earth in each century. In every hundred years it is estimated that the Earth is struck approximately three times by meteorites weighing several hundred tons. In the present century two huge meteorites landed in Russia; one, in Siberia, felled trees up to a distance of 80 kilometers. Many centuries ago a meteorite landed in Arizona and formed what is now known as the Barringer Crater. The crater has an average diameter of 1,200 meters.

Cometary Particles

The cometary particles are estimated to constitute more than 90 percent of the total influx of particles which enter the Earth's atmosphere. The large relative percentage of cometary particles counted, compared with the astroidal particles, may be influenced somewhat by the photographability of each type. As is discussed subsequently, there is some evidence which indicates that the cometary particles are of low average density, quite porous, and frangible. These characteristics are favorable for the production of a flaring meteor or one which, at some point along its path, is quite bright and is more easily noticed than a nonflaring meteor.

A present hypothesis is that comets are formed by a gradual accumulation of atoms and particles which are wandering randomly in space. It is estimated that our Sun is capable of maintaining 10^{11} comets in a solar orbit (ref. 12), the majority of which are great distances from the Sun. Occasionally one of the comets may be disturbed by a passing star and deflected toward the Sun. If the comet passes within 3 astronomical units of the Sun, it can be viewed from the Earth. (One astronomical unit equals the average radius of the Earth's orbit about the Sun.)

A comet which originates at great distances from the Sun will have a nearly parabolic orbit. Under the proper conditions, as the comet nears the Sun, the influence of the planets can be such that the comet will become a permanent member of the solar system and will reappear in a periodic fashion. On the average, several "new" comets are discovered each year; of course, one cannot be certain that these are really new, or if they are instead long-period comets whose previous arrivals have not been recorded.

On the other hand, comets are lost from view as a result of two major effects. The comet may pass closely enough to a large planet to be influenced by its gravitational field, which may deflect the comet so that the new orbit precludes the proper relationship between the comet-Earth-Sun system to permit

observation; the comet may remain too far from the Earth to be seen, or may not be properly illuminated by the Sun to permit detection. The other important effect is one of destruction which occurs as the comet passes through perihelion (closest distance to the Sun); the Sun's warming effect, gravitational pull, and radiation pressure combine to disrupt the nucleus and scatter the constitutents.

A widely accepted concept is that a comet is not a very dense mass, but is instead a loose accumulation of particles. When comets pass between the Earth and the Sun they do not interrupt solar observations. It was originally thought that a comet was a sort of flying gravel bank, but in recent times this concept has been displaced by Whipple's comet model, which visualizes the comet as an icy conglomerate wherein frozen compounds bind mineral particles together. The low average density of a comet was demonstrated when a comet passed between Jupiter and one of its moons; the comet exerted no perceptible perturbation to the planet's trajectory nor did it influence the orbit of the moon.

As the comets pass between the Earth and the Sun, it is possible to make spectrographic analyses of these bodies and to obtain information on the chemical composition of the comet. Table I (from ref. 12) is a table of elements most commonly found in the solar system. It has been found, with the possible exception of helium, that comets are also made of these most common elements. Because the equilibrium temperature of objects in space at great distances from the Sun is intensely cold, many of the usual gaseous elements are in solid form, but it is not cold enough to freeze helium or molecular hydrogen. However, hydrogen can combine with oxygen and carbon to form compounds such as H_2O (water), CH_4 (methane), NH_3 (ammonia), CH_3COOH (acetic acid), and HCN (hydrocyanic acid). The freezing temperatures of these compounds are so high that they would exist as frozen ices at locations beyond the orbit of Saturn. The remaining mineral elements, such as magnesium, silicone, iron, sulphur, sodium, calcium, nickel, and aluminum are frozen within the ices.

As comets approach perihelion, the increase in intensity of radiant solar energy causes the frozen elements to change from ices to gases. The liquid phase is obviated by the low pressures of the space environment. Once the ices are gone, the nonsubliming mineral elements may be left in a fragile porous matrix of extremely low average density. This residue would remain in the same orbit as the original comet except for the scattering caused by the various perturbing forces which act upon the particles with nonuniform effect. (These perturbation forces will act upon all particles, whether of cometary origin or not, and are described in the section entitled "Pertubation Forces.")

It is suspected that none of the meteoritic objects yet found on the ground are of cometary origin. Jacchia (ref. 13) has analyzed a number of photographed meteors which flared suddenly. He concluded that a logical explanation for the sudden increase in brightness (or flaring) was that the single meteoroid was shattered into myriad fragments, each of which generated a small meteor. The camera could not resolve the individual meteors, but instead registered the integrated effect of the glowing cluster. By observing the altitude and velocity at which the flares took place, Jacchia found that a dynamic pressure of only

one-fiftieth of an atmosphere was sufficient to fracture the meteoroid. It was concluded from these observations that the cometary particles are extremely frangible.

When the Earth passes through the orbital path of a comet, meteor showers are frequently encountered. Even though a comet has been nearly destroyed because of too many successive passes in the proximity of the Sun, the nonsubliming residue of the comet continues in approximately the same orbital path. The perturbing forces cause a widening of this path, but the majority of the nonsubliming material remains concentrated in the orbit that the comet would have occupied if it had not vanished. One of the more spectacular periodic meteor showers of modern times - the Leonids - was identified as such in 1833. Since then it has occurred at nearly annual intervals, although the intensity varies greatly from year to year. In 1799 the intensity was high, and this intensity has been noted in intervals of about 33 years except in 1899 and 1932. It seems that the particles are scattered around the orbit, but are more concentrated in some parts of the orbit than in others. The paucity of the shower in 1899 and in 1932 was caused by the planet Jupiter; the denser part of the swarm has been influenced by Jupiter's gravitational field and has been deflected so that it no longer will pass through the Earth's orbital path. There is no doubt that the Leonids originated from a comet that was first observed in 1866; the comet moved slightly ahead of the densest part of the meteoroid region.

Many other meteor showers have been associated with particular comets (ref. 3). If the velocity and orbital direction of an individual meteor were closely defined, it is felt that nearly 70 percent of the incoming meteors could be classified as belonging to streams, although some streams would be broad with widely separated particles. At present about 30 percent of the incoming flux is associated with particular streams, and the remainder is classed as "sporadic" and is commonly treated as occurring randomly. Some recent experimental measurements of the meteoroid population (ref. 14) lead to a slightly different description of the environment.

Figure 1 (from ref. 15) illustrates the meteoroid "stream" model which is a concept partly inspired by the radar-observation data in reference 14. It is assumed that all meteoroids are members of streams. The stream intensity may be great or small. The fact that during some periods the observed meteors seem to have a rather random direction is explained by assuming that the earth is usually simultaneously immersed in a dozen or so streams. The observed intensity fluctuations of identified periodic streams (such as the Leonids) occur because the earth does not always pass through the central core of the stream (or because the average stream flux has changed). Thus, instead of classifying meteoroids into "streams" or "sporadic" groups, all meteoroids are considered to be related to streams, and the streams are classified as "periodic" (usually intense) or "sporadic."

In either case, the concept used to describe the meteoroid population is a matter of mathematical convenience. For other than the known meteoroid showers, a statistical or "random" description will probably be used to predict the meteoroid-flux rate for a given period.

Tektites

Tektites are mineral objects of speculative origin which have been found in a few localized parts of the world. The chemical composition of tektites is approximately 65 percent SiO_2 and about 18 percent of the remainder is Al_2O_3. The ratio of iron-to-nickel content is about 500 to 1. The physical form resembles glass, as if the tektites at one time had experienced intense heat. The hypotheses on the origin of tektites are divided into two classes: (1) tektites have a terrestrial origin, and (2) tektites have an extraterrestrial origin. The first known mention of tektites appeared in the scientific literature in 1787.

The argument for terrestrial origin (see ref. 16) attributes the glassy physical form to intense heating caused by either volcanic activity or by a meteorite which struck the Earth's surface at high speed. The intense heat during either of these conflagrative activities melted the stones which were then thrown into the air by the volcanic explosion or the meteorite impact. The stones scattered and cooled during passage through the atmosphere. The outside cooled and hardened first; subsequently, subsurface voids were formed as the interior cooled and contracted. The high ratio of iron to nickel in tektites is unusual for meteorites; meteorites have commonly exhibited an iron-to-nickel ratio of about 20 to 1. A ratio closer to 20 to 1 rather than the 500-to-1 ratio found in tektites would be expected if the tektites were of extraterrestrial origin. Also, tektites show a very low degree of cosmic bombardment, which indicates that they were protected by the Earth's atmosphere after they achieved the glassy form. If tektites arrived as a meteoroid shower from space, they should be found on the ground in a band around the Earth; instead, they are found in patches of about 50 to 100 miles in radius; some patches are near (within few hundred miles) each other and others are on separate continents.

The hypothesis for extraterrestrial origin is that the chemical composition of tektites does not resemble the other mineral forms in the areas in which tektites are found. The tektites contain bubbles within which a good vacuum exists; this is taken to indicate that the bubbles might have been formed under fairly high vacuum conditions such as those at about 60 miles above the Earth. Radar and polarized-light reflectivity measurements on the Moon's surface show that the chemical composition of the surface could closely resemble that found in tektites. The glassy form could be a result of an Earth satellite which entered the atmosphere at fairly low inclination and which experienced aerodynamic heating.

Recent hypervelocity ablation experiments with tektite glass have produced in the laboratory models accurately resembling Australian tektites. The overall evidence in reference 17 indicates that australites are objects which entered the Earth's atmosphere as individual pieces of rigid glass and were shaped by severe aerodynamic heating. Machine calculations have shown that such an orbit is possible and that the localized character of the tektite "finds" can be explained by the atmospheric entry of one or more large objects which broke up in the atmosphere. The hypothesis is that some object was chipped from the Moon, became a natural temporary Earth satellite, entered the Earth's atmosphere, and broke into several large pieces which were heated to about 2,000° F to create the glassy form.

Because of their relatively rare occurrence, tektites are not considered to be a hazard to space vehicles.

Perturbation Forces

The perturbation forces acting on the particles, the comets, and the asteroids, can be divided into two groups. The first group is independent of the size of the particle, and the second group has a greater effect on the smaller than on the larger particles. The first group includes particle collisions and the influence of the planet Jupiter. The second group includes solar pressures, the Poynting-Robertson effect, erosion by collision, and the jet effect.

Forces independent of size.- As the asteroids and the comets travel through space they occasionally bump into one another. A common product of these collisions is smaller particles which, because of the impact, will diverge from the paths of the original bodies. Although the center of mass of the collision products may follow the same velocity vector as that of the original two-body system, the individual fragments will scatter.

The influence of the planetary gravitational fields has been mentioned previously. (See also ref. 18.) Jupiter, because of its large mass, has a great effect on the smaller bodies of the solar system which approach it. Over long periods Jupiter has influenced the motion of the asteroids, most of which travel in highly elliptic orbits between the orbits of Mars and Jupiter. This influence appears in the general tendency of the perihelia of asteroids to lie in the same direction as that of Jupiter. The largest eccentricities and inclinations are found for the asteroids with periods between 4 and 6 years (nearly half that of Jupiter). (See ref. 19.)

Effects which depend upon particle size.- The effects of some of the perturbation forces vary with the size of the particle. The solar pressure will act upon all particles. It has been demonstrated by calculation that the solar pressure is capable of blowing away all particles with diameters less than approximately 1 micron. As the particle size decreases, the ratio of the surface area to its volume increases; therefore, for a given density, the ratio of the surface area to the mass increases. The solar-pressure force is directly proportional to the area presented toward the Sun, and the imparted acceleration is inversely proportional to the particle mass. If it is assumed that a particle is not orbiting about the Sun and therefore has no inertial force which tends to hold it away from the Sun, this particle is then influenced only by the Sun's gravitational field and by solar pressure. Particles in the vicinity of the Earth which are 1 micron in diameter and have a density of that of aluminum are of the proper size for the solar pressure just to balance the force of the Sun's gravitational field. As this particle becomes smaller, its surface area increases with respect to its mass and the solar-pressure force then exceeds the force exerted by the Sun's gravitational field and the particle is blown away from the solar system.

The Poynting-Robertson effect is a relativistic phenomenon which imparts a drag force to the small isolated particles (with diameters on the order of 5 microns or somewhat larger) which orbit the Sun and is caused by the absorption and subsequent reemission of solar energy by the particle. It is assumed that the temperature of a given particle remains constant while it is in orbit around the Sun, and therefore all the radiant energy absorbed by this particle

from solar radiation must be reemitted. If a solar reference frame of coordinates is used, the reemission of energy produces a resisting force on the particle which is proportional to its velocity in orbit around the Sun. Over long periods of time this resisting force will reduce the semimajor axis and the eccentricity of the orbit of any small body, and ultimately the drag force will cause the body to spiral into the Sun. Wyatt and Whipple (ref. 20) have calculated that in 3×10^9 years all particles less than 8 centimeters in diameter will have been swept into the Sun by this effect. The fact that there are still particles of 8 centimeters in diameter and smaller floating around in space indicates that there is a continuous source of these particles.

A recent, as yet unpublished, study has been made by Whipple in an attempt to establish limits on the erosion rates of meteorites by collision with smaller meteoroidic particles. The computations used the spallation products of cosmic rays (argon ^{38}A and ^{39}A) in recovered meteorites to estimate the age of the meteorite, and thus the period of time over which erosion took place. Under the assumptions made, the calculations indicate that erosion is a greater cause of meteoroid destruction (or generation of smaller particles) than the Poynting-Robertson effect.

The jet effect is one which is peculiar to the cometary particles. Figure 2 is a sketch showing how this effect disturbs the trajectory of the particle. In this figure, two particles are shown - one which is not rotating and one which is rotating. Both particles are in orbit about the Sun. The particle in the lower right is subjected to solar pressure on one side - the side facing the Sun. However, it must be remembered that these cometary particles can contain large percentages of the mass as ices. The ices on the side toward the Sun will be warmed more than the ices on the side away from the Sun. As the ices sublime, the gas that is driven off is predominantly in the direction of the Sun. A momentum is imparted by these gases (in a manner similar to a small rocket motor) which adds an additional impulse to that provided by the solar pressure. The net impulse, then, is larger than that due to solar pressure alone. The particle shown in the upper right of figure 2 is spinning about its own axis in a counterclockwise direction as it turns about the Sun in a counterclockwise direction. Because the particle is spinning, the point of maximum surface temperature does not directly face the Sun. Due to thermal lag the maximum temperature occurs after the point has passed the position of receiving the highest heating rate. The maximum amount of gas will be driven off at an angle to the direction to the Sun, and will have a resultant-force component in the direction of the velocity. An oppositely rotating particle will have a retarding component. Since the rate of spin, rate of sublimation, and particle mass would be different for a randomly selected group of particles, the jet effect tends to scatter the swarm.

Observations of Meteors From the Earth

Photographic.- Until the past 15 years the main method of gathering data on meteors was that of visual observation. Trained observers were stationed at various points around the Earth to count meteors which could be seen with the

naked eye, and to try to estimate the meteor altitudes and trajectories. In the past 20 years or so, it has been possible to use cameras instead of individual observers. The obvious advantage is that a camera gives a permanent record which can be studied at leisure and which provides much more accurate measurements of trajectories. An initial program was attempted at Yale University using two cameras which photographed the same portion of the sky simultaneously; however, the base line separating these two cameras was too small to provide accurate triangulation measurements. Subsequently, Whipple, at Harvard, established a two-camera observation system separated by a base line of approximately 40 km. A new Whipple camera system using Super-Schmidt cameras has been located in New Mexico, where the average weather conditions are more suitable for astronomical observations than the weather at Harvard (Cambridge, Mass.) The Super-Schmidt cameras are capable of recording fainter meteors than the original cameras. This system also uses a base line of 40 km. A calibrated rotating-shutter system periodically interrupts the meteoric light path; the lengths of the interrupted traces on the film plates are measured to obtain velocity information. Triangulation is used between the two cameras to obtain the particle altitudes and trajectories.

The brightness of incoming meteors is measured on the visual magnitude scale, which is logarithmic. As the numbers on the visual magnitude scale increase, the brightness of a given body decreases. The zero value for the visual magnitude scale is taken as the average brightness of certain stars. (A star of zero magnitude is as bright as one standard candle viewed from a distance of 1 km.) On this scale the Sun has a visual magnitude of approximately -26.7, and the full Moon, -12. At present, the cameras in use can record meteors as faint as visual magnitude +5, which is also the brightness threshold for naked-eye observation. The ratio of the brightness intensity I between two given steps on the visual magnitude M scale is

$$\frac{I_1}{I_2} = 10^{-0.4\left(M_1 - M_2\right)} = 10^{-0.4\Delta M}$$

In addition to the brightness measurements, about 200 photospectrograms of meteor trails exist. Although these spectrograms reveal the qualitative composition of the meteoroids, no quantitative measurements can be made until some means of calibrating the spectral luminosity of the meteor can be developed.

Radar.- The photographic data have been augmented by data supplied by radar. A particle which enters the Earth's atmosphere generates a trail of ions. Radar beams can be bounced from this trail to obtain the velocity and some limited trajectory measurements of the meteor. The advantage of the radar (and also the radio observations) is that these are unaffected by the sunlight or moonlight, whereas the photographic observations are possible only during clear, dark, moonless nights.

The radar technique has been so improved that it is now possible to detect particles of a size which is equivalent to a +10 visual magnitude meteor. A high-efficiency transmitting antenna is being used in conjunction with six receiving antennas; this system permits the determination of the trajectory from which the original meteoroid orbit can be calculated. (If high-efficiency

receiving antennas be installed on the receivers, the sensitivity of this particular system could be increased by another two orders of magnitude.) It is also possible to record some of these data automatically. (It is believed that, with some development work, a radar sensitive to +16 visual magnitude can be built.)

Radio.- Radio measurements by themselves are only counting devices and do not determine meteor trajectories without supplementary information as do the photographic and radar measurements. The ionized trail of an incoming meteor, in conjunction with a radio transmitter, generates a so-called whistle by a beat-frequency effect. Automatic instrumentation has been set up to record these whistles. Radio systems are used to get indications of meteoroid flux.

It has been found that the radio and radar measurements are somewhat sensitive to the frequency used. A given frequency will be more sensitive to a meteor of one size than another, and thus radios at different frequencies will count different numbers of particles, even though both radio systems observe the same portion of the sky. This originally presented some difficulty in correlating the results of measurements made at different frequencies.

Meteor flux distribution.- Figure 3 shows some results from radar observations. This figure is a polar plot of the observed and actual flux of particles at the Earth's distance from the Sun and is a yearly average of all particles. Two surveys were made; the solid line is faired through data obtained in 1949-1950, and the dashed line through data obtained in 1950-1951. The motion of the Earth affects the apparent direction from which the meteor originated; the actual flux is obtained by correcting for the influence of the Earth's orbital motion. It can be seen from this figure that the apparent influx is greatest in the morning hours and on the side of the Earth facing the Earth's motion about the Sun. Therefore, the Earth is running into a great number of particles; however, once corrections are made for the Earth's velocity through space, it is found that most of the particles are traveling in the same direction as the Earth. Figure 4 shows that most of the incoming particles have trajectories at small angles with the plane of the ecliptic, which is the plane determined by the Earth's orbital motion around the Sun. More than 90 percent of the particles are included within 40° of this plane; this is not surprising because most of the comets which are seen from the earth also come in within 40° of the ecliptic plane. Such a correlation supports Whipple's hypothesis that meteoroids have a cometary origin. Although the spatial and temporal variations of the meteoroid influx have been mapped by the use of radar and radio methods, cameras have supplied most of the information by which the variation in influx rate as a function of particle size can be determined. Table II lists the influx rate for particles of various mass.

Accuracy of meteor observation systems.- A major experimental uncertainty is common to all three observation systems. None of the particles observed by the systems have been available for subsequent scrutiny in a laboratory. All have been destroyed or lost in transit through the atmosphere. Although it may be possible to correlate the data from different devices, the utility of the information is hampered by the lack of an absolute standard. Factual data on the mass, size, shape, aerodynamic drag, density, and luminous efficiency of the

meteoritic particles is sorely lacking, and thus the characteristics of the meteor-causing particle are actually unknown. Reference 21 contains equations used in the analysis of data acquired from photographic observations. Estimates of the mass and density of the meteoroids have been deduced by assuming a number for the luminous efficiency. The accuracy of and confidence in the data would be greatly enhanced if any of the following meteoroid characteristics were known: the mass, the density, or the luminous efficiency.

Estimates of meteoroid flux density.- Whipple's 1957 table will be taken as the basic table for comparison purposes in this paper. It is noted at this point that if this table be used in conjunction with the more recent conservative penetration theories to estimate the meteoroid threat to a circumlunar vehicle, the necessary meteoroid protection system will incur a severe weight penalty.

The data from table II are plotted in figure 5, along with similar data presented by Watson (ref. 18). These two curves represent the extreme of the estimates of the influx. Also shown in the figure are data points obtained from satellite experiments. Whipple's photographic data were obtained in the upper mass range at about 10^{-1} grams; the satellite experiments are in the low-mass range (for reasons which will be discussed in the section entitled "Satellites and Space Probes"). The "no-man's land" in between coincides with the range of interest to the structures designer.

The values shown in the mass column in table II are in a state of revision. Early experiments by McCrosky (ref. 22) in programs similar to Project Trailblazer indicate with a good probability that the numbers in the mass column are high by some factor between 3 and 200 (the values in the mass column of table II represent the highest estimates made to date). Whipple, in a recent paper (ref. 23), discusses briefly the determination of the mass in table II. Of the possible values for the mass, Whipple chose the highest for reasons of safety in engineering calculations; the values chosen may be high by an order of magnitude. The critical factor is in relating the mass of the meteoroid to the observed brightness of the meteor.

Öpik (ref. 24) rather comprehensively discussed the various aspects of meteor physics. He arrived at the following equation for the relationship of mass to brightness:

$$\log_{10} m = 10.02 + \log_{10} l - \log_{10} \beta - 3 \log_{10} V - 0.4 M_0$$

where m is in grams, l is the length of the meteor train in centimeters, V is the velocity in centimeters per second, and M_0 is the visual magnitude of the meteor, and β is the luminous efficiency.

The factor β is composed of

$$\beta = \beta_0 + \beta_\theta + \beta_\lambda$$

where β_o is the luminous efficiency of meteor vapors which are ionized and excited during the conversion of kinetic energy to visible light, β_θ is the luminous efficiency associated with thermal collisions between atoms in the coma (the jet of vapor atoms which emerge from the meteoroid and mix with the air), and β_λ is the component associated with blackbody radiation of the hot meteoroid surface.

The evaluation of the various ingredients contained in β is not a simple process, and estimates of β differ by an order of magnitude. One of the purposes of Project Trailblazer is to produce artificial meteors by firing pellets down into the Earth's atmosphere (from a rocket nose cone) at velocities above the lower limit of the meteoroid range (11 km/sec). The pellets are of known size and chemical composition. The atmospheric entry of the pellets is observed with cameras. The luminous efficiency of the conversion of kinetic energy to visible light can be calculated because the characteristics of the simulated meteoroid are known. Several experiments, using different materials for the pellets, will probably be required because of the complex chemical constituency of a meteoroid. It is noted here that the luminous efficiency estimated by Öpik is somewhat higher than that utilized by Whipple in computing the masses in table II.

The radii greater than 39.8 microns in table II were computed by assuming a spherical particle with a density of 0.05 g/cm^3. It was necessary to increase this density gradually for particles smaller than 3.96×10^{-8} grams in order to reduce the ratio of surface area to mass, otherwise the solar pressure would exceed the Sun's gravitational pull and the particles would be blown from the solar system. Öpik (ref. 25) has estimated that the average density of the puff-ball meteoroids might lie between 0.01 and 0.1 g/cm^3 on the theory that the porous meteoroids are of grainy construction, and by using the density of stone (3.5 g/cm^3) he estimates the radius of the individual dust grains in the puff ball to be between 200 and 300 microns. According to Öpik, any particles smaller than this will be of stony density. However, Whipple feels that the present (1961) evidence indicates that even the very small sizes are of the porous nongrainy structure. McCrosky has used data from the Trailblazer program and the Harvard meteor program to compute an average density of about 1 g/cm^3 (which might be accurate within a factor of two).

Whipple's 1957 table was developed by observing photographic meteors down to visual magnitude +5 and was extrapolated to visual magnitude +31 by assuming that the mass influx in each magnitude step is a constant; that is, as the sizes of particles decrease, their frequency increases. The number of impacts per square foot column is a cumulative number; this column is a summation of all the particles of a given mass and greater striking the square-foot area. This frequency column was computed from Whipple's original table which showed the average cumulative number of particles striking the earth per day.

Analytically, the mass distribution of individual particles can be computed from the visual magnitude from

$$m = K_1 10^{-0.4M} \qquad (1)$$

where m is the mass, M the visual magnitude, and K_1 a constant. According to the previous discussion about the mass, the value of K_1 is very much in doubt, although, in time, it is hoped that K_1 may be determined to within better than an order of magnitude. A similar equation is given by Whipple (ref. 23) to relate the number of impacts per square meter per second N to the meteoroid mass m.

$$\log_{10} N = \alpha + \xi \log_{10} m$$

Included in reference 23 is a table of values of α and ξ as predicted from various sources.

Meteoroid velocities.- The velocity limits of particles which are observed from the Earth lie between 11 km/sec and 73 km/sec. The 11 km/sec value is determined by the velocity which a particle would have if, starting from rest, it fell from a great distance under only the influence of the Earth's gravitational field. The upper limit is based on the assumption that the Earth runs head on into a particle which is in retrograde orbit around the Sun, and is determined by adding the Earth's orbital speed to the maximum orbital speed of this retrograde particle at the Earth's radial distance from the Sun. Figure 6 (from ref. 21) shows the velocity distribution of meteors corrected for atmospheric drag. Meteors from known large showers are indicated by a cross-hatched region. The figure was constructed from the photographic observation of meteors as bright as and brighter than +4.5 visual magnitude.

Satellites and Space Probes

Satellites have been used to supplement ground observations. Summaries of some of the satellite experiments may be found in references 26 through 32. The data points differentiate among three types of observations - (1) soundings which are made by rockets fired up to 100 or 200 kilometers, and which then fall back to Earth; (2) satellites which remain in relatively permanent orbit around the Earth; (3) Space probes from vehicles which have been sent out to very great distances from the Earth.

Recent data analyses have shown that, in the period within about 6 hours after launch, nearly all of the satellites apparently recorded very high particle flux rates. Subsequent ground tests showed that these suspicious counts were probably caused by the sensitive microphones recording the creaking of the satellite as it adjusted to its thermal environment in space. The more recent data have had this effect subtracted out.

Most of the particles were detected by microphones attached to sensitive surfaces on the satellite. In one case, wire-wound coils indicated impacts when the wire was broken. During the data reduction it was assumed that the microphone threshold was dependent solely upon the momentum of the impacting particle. In order to fix a minimum value of mass to a particle, it has been assumed herein that all particles struck the sensors at an impact velocity of 30 km/sec. The Russian satellite data (ref. 33) are indicated by the dark triangle in figure 5.

(The Russian data have been reduced on the basis that the microphones are sensitive to the amount of material spewed out from the crater caused by the impact, and that the electronic pulse depends somewhat upon kinetic energy (see ref. 34).)

Previous flight experiments have not determined the flux rates of particles large enough to puncture space vehicles. The sensitive microphone areas necessarily have been small. Because these areas were small, the microphones were made quite sensitive in order to record at least a few impacts. (It will be recalled that the lighter particles are more abundant than the heavier particles.) It was necessary that a fairly large number of counts be recorded in order that the satellite data have statistical significance. The question of statistical significance and the design of satellite experiments is discussed in reference 11.

The space-vehicle data determine the line shown in figure 5 through the data points. This line does not have the same slope as the lines extrapolated from the photographic and radar observations. The two methods of detection are, of course, different, and both suffer from a lack of dependable calibration; the photographic data need a reliable evaluation of the luminous efficiency and the radar data need sensitivity calibrations, while the space-vehicle microphone sensitivity has not been measured by using particles traveling at meteoric speeds. If the space-vehicle measurements be considered reliable, it then appears that there might be a concentration of dust in the vicinity of the Earth. Whipple (ref. 31) has hypothesized that there is a dust cloud in the vicinity of the Earth consisting of particles which are in Earth-centered orbits. This implies a dependence of the frequency of impact upon the altitude of the vehicle. Supporting evidence has been noted in reference 29.

In reference 29 Soberman and Lucca note a discrepancy between the number of impacts counted by microphones and the number of wire-wound grid sensors broken. The number of microphone impacts was about that which would be expected from other satellite measurements, but the number of wire grids broken was zero on one vehicle (Midas II 1960 Zeta 1), and disproportionately small (8 out of 80 of very sensitive wire grids) compared to the microphone data on a second (Samos II 1961 Alpha I).

Soberman has also been associated with the Venus fly-trap experiment, wherein a recoverable rocket nose cone lined with plastic opened to sample the dust population during the apex of the rocket flight. The dust trapped by this rocket probably included many particles which were drifting at low velocities down into the atmosphere. The plastic was examined in an electron microscope and micron-sized holes were observed. The shape of the holes was taken to be indicative of the shape of the particle. Soberman has excellent photographs (ref. 32) which show jagged and irregular holes, and also almost perfectly circular holes.

From the results of the Midas II and Venus fly-trap experiments, Soberman concludes that, because few sensitive wire grids were broken during sampling of an apparently normal meteoroid dust flux, and because many particles appear to be jagged and irregular, the particles are physically frangible and shatter

easily upon impact. It is noted here that the wire-grid area exposed was small and the results will probably need to be confirmed by future experiments.

The previously discussed experiments generally employed instruments which counted impacts on a highly sensitive surface. One satellite experiment has been attempted whose express purpose was to measure the actual penetration flux through metals. In the design of space vehicles there is a need for data on the actual amount of damage meteoroids can cause, and experiments which measure penetration directly circumvent the need for accurate evaluation of the amount of damage which can be caused by a meteoroid striking a space vehicle at extremely high relative velocity. Explorer VIII (1960 Xi 1) (also called the S-55A) carried pressurized semicylinders of beryllium copper, with wall thicknesses ranging from 1 to 5 mils; upon puncture, the pressure loss actuated a switch to record the event. Stainless-steel sheets (3 to 6 mils thick) backed with a current-carrying gold-foil grid detected punctures when the grid was broken. Cards wound with thin wire detected meteoroids if the wire were broken. Impact microphones and cadmium-sulphide light detectors were also carried. A description of the satellite instrumentation may be found in reference 35.

The useful lifetime of the satellite was 2 days. The impact microphones registered a dust impact rate which was only slightly higher than that measured by microphones on other satellites. However, there were no punctures of the pressurized cans, nor were any of the foil-backed stainless-steel panels punctured. If Watson's estimate (ref. 18) of the meteoroid flux be correct, there would be about a 0.5 probability of achieving these results. If Whipple's 1957 estimate (which predicts a greater number of particles of a given mass) be correct, the probability of having no punctures is near zero. Therefore, during the experiment period, it can be concluded that the puncture rate was probably closer to that which would be predicted from the less severe estimate of the meteoroid hazard.

Both of Soberman's experiments with the wire-wound cards and with the S-55 satellite indicate that the penetrating flux is less than would be inferred from data obtained by the microphones which detect particle impact.

One aspect of the meteoroid environment has been ignored to too great an extent in all previous calculations of the probability of occurrence. Both radar observations (ref. 14) and the satellite microphones have shown that the meteoroid flux rate is not constant. This nonconstancy is evident, even after the effects of the visible large-particle showers have been subtracted from the data. The variation in flux rate is of one or two orders of magnitude with periods of high or low intensity of a few days duration. The variation apparently occurs randomly, except for the known visible meteor showers and a known general annual variation whose maximum occurs during the summer months. The known variations can be taken into account easily; however, the random variations must, at present, be dealt with on a statistical basis.

Because the random variations seem to have periods of only a few days, a vehicle in space for a matter of weeks will probably encounter close to an average rate; conversely, a short-lived space vehicle may encounter a meteoroid flux considerably different from the average. These variations are apparent from the

wide range in flux shown by the radar data which took 5-minute-period samples, and the satellite data which generally is an average rate for a several-day period. Too little is known about the statistical variations in meteoroid flux to predict short-time impact results, but the existence of these variations must be recognized in interpreting the satellite data. The interception of a meteoroid by an impact sensor depends not only upon the chance of intercepting a meteoroid of a known flux intensity, but also the chance that the flux intensity is a certain value during the sampling period.

Research in Progress

Research in progress on the determination of the properties of the meteoritic particles in space is known to include the projects listed in table III.

INTERACTION BETWEEN METEOROID ENVIRONMENT AND STRUCTURE

The immediate result of meteoroid impingement on a vehicle structure is local damage of a very special character. Consideration in this section will be restricted to the local effects, not to the total damage or end result which may affect large portions of the vehicle and its mission.

Although the laws of chance indicate that a space vehicle will be struck by particles with masses much less than 1 gram, the high velocity of impact of 15 or more kilometers per second can result in either definite surface damage or complete penetration of the vehicle wall. Much theoretical and experimental work is under way in an attempt to discover the laws governing the process of hypervelocity impact cratering and penetration. Usually the results of these investigations are published individually. Reference 10 is an excellent survey of hypervelocity impact information, in which an attempt has been made to bring together in one report the data from many individual investigations. Reference 10 also includes a correlation analysis between various forms of the theoretical impact equations and experimental data. The discussion of the hypervelocity impact phenomena which follows is largely based on material compiled by Herrmann and Jones.

Historical Aspects of the Plate Perforation Problem

Work on the penetration of targets by rigid projectiles was started by Robins in 1742, and his ideas were later elaborated by Euler, both in theory and experiment. Work carried out since then until recent times has been for engineering purposes, in which the resistance to penetration has been represented by certain dominant features determined by an assumed penetration model with parameters fixed by experiment. In the earliest studies, and in recent simplified theories of armor penetration, the projectile is considered to be rigid. The Euler-Robins theory (ref. 36) assumes a constant resistance to penetration, in which case

$$\frac{1}{2} m_p V_L^2 = K\pi R^2 t$$

$$V_L = 2\pi K t^{1/2} \frac{R}{m_p^{1/2}}$$

where V_L = maximum velocity for complete penetration, m_p = mass of the projectile, R = radius of the projectile, and t = thickness of the plate.

Early experimental work indicated that the resistance force varied as the product tR, and the work done in perforation as t^2R, so that the projectile velocity for perforation was given by

$$V_L = \frac{KtR^{1/2}}{m_p^{1/2}}$$

The proportionality constant K, however, varied considerably even for small changes in velocity. On the assumption that the resistance force varied as tR/V, Tresidder obtained the relation for wrought iron

$$V_L = 10{,}140 \frac{t^{2/3} R^{1/3}}{m_p^{1/3}}$$

Similar expressions with different fractional exponents and values for the constant are still in widespread use today in the design of armor plating.

These relations are applicable to plate penetration when the projectile remains essentially intact, but are of no use at higher velocities when the projectile disintegrates. Nevertheless they are frequently seen to influence the contemporary study of hypervelocity penetration.

Physical Description of High-Speed Impact Phenomena

Observational data.- High-speed optical and X-ray photography have made it possible to observe the actual process of high-velocity cratering and penetration. When this qualitative information is taken together with information gathered in many related fields of flat-plate impact and spallation, explosive loading and forming, and current theoretical understanding of wave propagation, it is possible to construct a fairly detailed picture of the phenomena attending cratering and penetration. This phenomena will now be described in this section without any attempt to indicate the source of the information used.

The stress field set up by impact.- Upon impact, stress waves originate at the pellet-target interface and move into the target ahead of the pellet-target interface, and back into the projectile. These stress waves are clearly more intense than elastic waves, and move at a velocity dependent on the magnitude of the pressure increase across the wave. For increasing pressure jumps the wave velocity varies from less than to greater than the elastic wave velocity. In laboratory coordinates fixed on the target, the wave propagating into the target will move at a velocity equal to or greater than the velocity of the pellet-target interface. The pellet-target interface will move at a velocity less than the incident pellet velocity; this velocity is dependent upon the densities of the pellet and target material. The wave propagating back into the pellet may move at a velocity greater than or less than the incident pellet velocity, and thus in laboratory coordinates propagate upwards above the original surface of the target or propagate below the surface of the target.

After the initial impact period, rarefaction waves will sweep in from the free surfaces as a result of reflection of the compression waves at the free boundaries attenuating the initial waves, and inducing lateral motion in the pellet and target material.

The wave propagation picture is greatly complicated by the fact that the materials involved can support shear stresses. Thus, there will be elastic waves,

dilatational and shear waves, and the stresses at a point in the material will not be the same in all directions, as in the case of a fluid.

Conventional armor penetration.- In the following descriptions of the penetration processes, a cylindrical projectile will be assumed for illustrative purposes, although the description applies also to the projectiles of other shapes. At very low velocities, the speed of penetration is sufficiently slow so that the waves reverberate across the target plate and the projectile many times during the penetration process. The in-plane stresses which are set up are sufficiently low so that only elastic deformations occur in the plane of the plate surface. The projectile is undeformed and a plug is sheared out of the plate.

In thin targets, the target often deforms quite severely, and instead of a plug being punched out of the target, the target stretches, fails in tension, and a series of petals results. However, at higher velocities, the inertial forces prevent such gross motion of the target, and plugging-type failures again occur.

At still higher velocities, the stresses become so high that the induced in-plane radial stresses become greater than the elastic limit, and local in-plane motion of the target is initiated. The radial flow of target material causes a thickening of the target plate around the crater. This type of failure is known as ductile penetration. Clearly, combinations of plugging, petalling, and ductile failure are possible inasmuch as the boundaries between the regimes in which these failures occur are not clearly defined. The type of failure which predominates clearly depends both on the projectile velocity and the properties of the target, for example, shear strength, ductility, and hardness. However, in these regimes the projectile suffers only minor deformation.

High-velocity penetration.- A major change in the cratering mechanism takes place when the projectile breaks up. At sufficiently high velocity, the radial stresses induced in the projectile by the stress wave system become high enough to cause lateral flow of the projectile material. If the projectile is brittle, the projectile fractures, usually into many small pieces. The presented area of the shattered projectile is much greater than the intact projectile, and a consequent higher impact velocity is required to penetrate the same thickness of target. If the projectile is ductile, the projectile will flow and "mushroom" thereby increasing in diameter rather than fracturing, and a similar effect may be expected, although not so pronounced as for a shattered projectile.

At still higher velocities, the stress waves may become so intense that on first reflection of the wave system at the rear surface of the target plate, tensile stresses greater than the fracture stress are produced, and pieces are removed from the rear surface of the target by spalling. This type of failure reduces the effective thickness of the target plate as a penetration barrier.

Hypervelocity penetration.- At very high velocities, the stress waves will, at least initially, be many orders of magnitude higher than the strength of the material, and the material (even if brittle under normal conditions) will flow like a liquid. Penetration will very likely occur in a time equal to only one reverberation of the stress waves through the target plate, and the projectile and the target material will be ejected both backwards and forwards as a spray

of small particles. Of course, for somewhat thicker targets, and for threshold penetration (where the velocity is just sufficient to cause penetration), the "fluid" phase will occupy only the initial part of the motion. The stress waves will rapidly attenuate to the degree where material strength again becomes important, and the final phase of the penetration may again involve spallation and the other more familiar modes.

For extremely high velocity impact, additional phenomena are encountered. Melting and/or vaporization of the projectile material may be caused by the residual heating due to the gain in entropy across the shock wave emanating from the projectile-target interface. As penetration proceeds and the waves attenuate to the point where material strength becomes important, this portion of the material will still act as a fluid as a result of its high temperature, with a consequent greater ejection of material from the developing crater.

For cases of threshold penetration, most or all of the above-mentioned phenomena may be involved. The initial portion of the motion most likely will be "fluid," some material may be melted and vaporized, attenuation of the stress wave system will lead to material strength controlling the subsequent motion, spalls may be ejected from the rear surface of the target, and the final stage of the penetration may involve a combination of plugging, petalling, and ductile penetration. Therefore, it is not clear at present, whether gross simplifying assumptions may be made for the hypervelocity penetration of thin targets. However, some fairly simple situations do exist which may involve only one or two of these phenomena as the major mode of failure.

Modern Theories of Penetration

Currently several simplified theoretical analyses of high velocity and hypervelocity impact exist. These may be classified in accordance with the assumptions made, which make them especially suited to some particular target-projectile configuration and velocity range:

(1) Rigid projectile (as in the case of armor perforation methods) with the target taken to be either elastic-plastic or fluid;

(2) Hydrodynamic projectile; that is, projectile of zero shear strength, with the target treated either as a fluid or with its material strength properties introduced as a correction factor;

(3) Thermal penetration, in which the available kinetic energy is equated to the heat of vaporization of the target;

(4) Explosive analogy, which neglects the projectile mass itself and considers only the energy release.

Rigid projectile.- For armor penetration and perforation, the projectile is usually assumed to be undeformed as a result of the impact. Actually it does deform plastically to some extent and a thin layer may melt. Several advanced

theories have been postulated to take better account of these effects, each for a different target behavior.

The Bethe theory (ref. 37) is developed for the case of a ductile, thick-plate target. Plane strain is assumed, the plastic-yield condition is defined by the Tresca-Mohr criterion, and an expression is obtained for the work required to expand a hole to the radius of the projectile in an infinite plate of thickness t. The static solution for radial stress as a function of deformation is modified to provide a dynamic correction factor for deformation; a correction of the material yield stress based on Orowan's relation for dynamic yield effect is introduced. The resultant energy equation becomes

$$\frac{1}{2} m_p \left(V^2 - V_o^2\right) = \pi R^2 t \left\{ \frac{\sigma_y}{2} \left[\log_e \frac{2E}{(5 - 4\mu)\sigma_y} + 1 \right] + 3.8912 \frac{1 + \mu}{(5 - 4\mu)^2} \rho_t \left(\frac{\pi}{2} \frac{VR}{l} \right)^2 \right\}$$

where V_o is the emergent velocity, σ_y is the yield stress, E is the elastic modulus, μ is Poisson's ratio, ρ_t is the density of target material, R is the radius of the projectile, m_p is the mass of the projectile, V is the initial projectile velocity, and t is the plate thickness.

Bethe also obtains a solution for a thin-plate target by applying his dynamic correction terms to G. I. Taylor's analysis (ref. 38) for perforation of a thin ductile plate:

$$T = \pi R^2 t \left[1.33\sigma_y + 0.9728\rho_t \left(\frac{\pi}{2} \frac{VR}{l} \right)^2 \right]$$

where T is the kinetic energy of the projectile.

Thomson (ref. 39) and others consider the case of a very thin ductile plate which develops large bending deformation which produces petalling. Under static load, the enlargement of a hole in a plate always involves this type of deformation when the hole diameter exceeds 7 to 10 times its thickness. The plate is drawn out into a funnel shape by a tangential tension equal to σ_y. By assuming a displacement configuration the same as in the static case, the work done in enlarging the hole is

$$T = R^2 t \left[\frac{\sigma_y}{2} + \frac{\rho_t}{4} \left(\frac{\pi}{2} \frac{VR}{l} \right)^2 \right]$$

The theory of Zaid and Paul (refs. 40, 41, and 42) considers the target to be of incompressible material having zero strength, and the part of the target not struck directly by the projectile is assumed to remain undeformed. In effect this assumes that the plastic wave will not have had sufficient time to radiate any appreciable distance. The velocity lost by the projectile during penetration is then expressed by identifying the momentum transmitted to the deforming plate material.

Grimminger (ref. 1) uses similar assumptions in considering penetration of a spherical projectile into a target of zero strength. He assumes hydrodynamic resistance with a drag coefficient $C_D = 1$ at velocities above Mach 5; that is, for projectile velocity more than five times the plastic deformation velocity. After the velocity is reduced below this value, additional penetration is assumed to occur according to the armor penetration formula

$$\frac{P}{R} = \frac{2}{3}\frac{\rho_p}{K} V^2$$

where K is a constant for a given target material. The total penetration is consequently

$$\frac{P}{R} = \frac{8}{3}\frac{\rho_p}{\rho_t} \log_e \frac{V}{5u_t} + \frac{2}{3}\frac{\rho_p}{K}(5u_t)^2$$

where ρ_p is the projectile density, u_t is the velocity of plastic wave propagation in the target material, and V is greater than $5u_t$.

Several other theories have been formulated for the semi-infinite target, which have not up to the present been applied to the plate perforation problem (where different boundary conditions exist). Apart from Zaid's theory (ref. 43), all these consider the projectile to be of zero strength. In Zaid's hypervelocity theory, penetration takes place by the erosion of a rigid target by a rigid projectile where the projectile and target are separated by a thin film of incompressible fluid.

Hydrodynamic projectile.- The initial pressures generated in hypervelocity impact are so much greater than the shear strength of the material that this may be neglected in comparison. It is for this reason that the approach which neglects the strength effect has been termed hydrodynamic. Theories which use this approach consider that the resistance to projectile penetration arises entirely from the pressure required to accelerate the target material. Some of the theories include a correction to allow for the strength of the material.

Incompressible material is much easier to handle, and for this reason, the incompressibility has been assumed in most approximate analyses. Further simplification is obtained by considering the motion to be one dimensional. However, since some of these theories really consider only the dissipation of the projectile, and neglect the inertial expansion of the crater after the dissipation of the projectile, they will give good agreement only for projectiles in a restricted velocity range and of relatively long lengths, that is, jets and rods. For craters formed by spheres and short cylinders, the inertial expansion of the crater after the projectile has been dissipated is of the same order of importance as the expansion due to the pressure of the projectile, and it is expected that these theories would grossly underestimate the penetration. In these simple approaches Birkhoff et al. (ref. 44), Pack and Evans (ref. 45), and Cook (ref. 46),

apply Bernoulli's theorem at the collision interface, that is

$$\frac{1}{2}\rho_p(V - u)^2 = \frac{1}{2}\rho_t u^2$$

where u is the constant penetration velocity. At this rate a jet or projectile is used up in time $\tau = l/(V - u)$, and the depth of penetration is

$$P = \frac{lV}{V - u} = l\sqrt{\frac{\rho_p}{\rho_t}}$$

Modifications to this simple relation to account for target strength are introduced by Pack and Evans (ref. 45) and by Rostoker (ref. 47).

In a similar theory, Öpik (ref. 48) includes an allowance for the radial expansion of the target material under the pressure expressed in a moving frame of reference, by using Bernoulli's equation. Inasmuch as the flow in this frame of reference is not steady, only an approximation is achieved.

Bjork (ref. 49) is the first investigator to make a real attempt to analyze the motion during penetration. In his approach, the strength of both projectile and target is neglected and an equation of state based on theoretical physics, but evaluated experimentally, is used. This equation relates the internal energy, pressure, and specific volume of the material. The problem solved by Bjork was for a cylindrical projectile $l/d = 1$, impacting normally onto a semi-infinite target. A numerical solution was obtained by means of the IBM 704 data processing machine. The machine representation is only fairly accurate inasmuch as a total space mesh of 25 by 25 cells is the largest that could be conveniently handled, however, the main features of penetration are displayed quite clearly. Bjork's theoretical results are represented approximately by

$$P = K\left(m_p V\right)^{1/3} \qquad \text{meters}$$

where $K = 6.06 \times 10^{-3} m^{2/3}\text{-sec}^{1/3}\text{-kg}^{1/3}$ for an iron projectile and target, and $K = 10.9 \times 10^{-3} m^{2/3}\text{-sec}^{1/3}\text{-kg}^{1/3}$ for an aluminum projectile and target.

Despite the lack of accommodation for certain material properties (strength, work hardening, etc.) in the Bjork theory, it serves as a reasonable first approximation for theoretically predicting cratering under hypervelocity impact.

Thermal penetration.- In the thermal penetration theories that have been formulated, penetration is assumed to take place by the melting of the target by the projectile as it gives up its energy. Whipple's penetration theory (ref. 2) assumes that the crater formed by melting is a right-circular cone for which the total apex angle is 60°. By assuming that all the initial kinetic energy is converted into heat, the equation for the depth of penetration below the original surface can be written as

$$P = 10^{-2}\left(\frac{9T}{\pi\rho_t\zeta}\right)^{1/3} \quad \text{meters}$$

where ζ is the amount of energy required to raise 1 kilogram of target material from the initial target temperature to the melting point plus the latent heat of fusion.

Langton's theory (ref. 50) is similar to that given by Whipple, except that the crater is assumed to be hemispherical. For this theory, two cases are considered:

(1) the target melts but the particle does not

(2) both the particle and the target melt

The same theory, except that a cylindrical hole is assumed, has been used to compare with data obtained for the perforation of plate targets in reference 51.

Lavrent'yev's theory (ref. 52) of thermal penetration analyzes dissipation of the projectile energy within the target and assumes an incompressible medium which flows at a rate related to the distance from the projectile. This rate is obtained by assuming that momentum is conserved. The crater size is determined by assuming that all the kinetic energy is transformed into heat and that the material from the crater has been vaporized.

Explosives analogy.- In the theory, suggested by Rinehart and Pearson (ref. 53) and Stanyukovitch (ref. 54), the effect of the impinging projectile is represented by an explosive charge which is equivalent in caloric content to the kinetic energy of the projectile. The pressure level and shock waves produced on detonation and the resultant behavior of the target material are predicted by existing explosives theories.

Experimental Data

Considerable data have been reported both on the dimensions of craters produced in semi-infinite targets and on the damage to thin targets by projectiles traveling at velocities up to about 30,000 fps (9 km/sec). However, the great bulk of the data (obtained with light-gas guns) is for velocities at about 12,000 fps. (See refs. 55 through 64.)

Acceleration methods.- Various types of apparatus have been employed to accelerate projectiles to velocities up to 30,000 fps. The most widely used have been guns of a sort which use explosives to provide the initial driving energy. Guns are limited velocitywise because the projectile cannot travel faster than the shock wave created by the explosion, otherwise the projectile would outrun its driving force. In a simple gun, the shock-wave velocity is determined by the characteristics of the gases formed from the reaction of the explosive chemicals; the shock-wave velocity is higher in light gases like helium or hydrogen than in such products of combustion. Thus it is advantageous to introduce a light gas

between the primary explosive charge and the projectile. The light gas is compressed by an explosion-driven mechanical piston or by the explosive-gas shock wave itself. Recently, considerable interest has been shown in light-gas guns in which a high-joule electric arc is discharged through the light gas to supply additional energy (ref. 55). Extensive developmental work is being continued on light-gas gun techniques because such guns can deliver a projectile of known size and shape to the target. The projectile can be accelerated in a sabot (cradling container) which protects it from damage during passage through the gun barrel. After leaving the barrel, the projectile and sabot separate and the sabot, which is designed to deviate from the flight path, is captured by a system of baffles.

Another common method of obtaining high-speed particles is the use of shaped explosive charges. In this case the velocity limitations of the explosive gases are overcome by preferential momentum interchange which occurs upon implosion into a partially enclosed cavity. In the lined-cavity charge (developed for armor-piercing weapons), detonation of the explosive charges collapses a conically shaped metal liner. The kinematics are such as to produce, on the axis of the cone, a high-velocity jet of molten metal or metal fragments and a low-velocity slug. Theoretically the speed of the initial portion of the jet can be increased indefinitely at the expense of mass distribution between jet and slug by decreasing the angle of the cone. Practical limitations, however, are of the order of 10 km/sec, although values as high as 90 km/sec have been reported. The technique identified as the air-cavity charge uses a cylindrical cavity and no liner; a disk-shaped projectile, which is placed at the open end of the cavity, is accelerated by the jet of high-velocity gases. Velocities in the 5 km/sec range have been obtained with projectiles varying up to 10 grams in size. Because of low cost and versatility this method has become widely used, despite limitations on projectile shape and some difficulties with mass loss due to erosion. Several other shaped-charge techniques have also been reported (refs. 56 and 59).

Electrostatic accelerators are theoretically capable of accelerating tungsten spheres 1 micron in diameter to 80,000 fps. Iron particles with 1-micron radii have been projected at 30,000 fps. The particle velocity is a function of ratio between the charge on the surface and the mass, thus larger particles cannot be accelerated to as high a velocity as the smaller ones. A particular problem posed by this technique is to obtain a high proportion of the maximum theoretical charge on the particle. The iron particles had approximately 10 percent of the maximum theoretical charge, while the previously mentioned tungsten particles would require at least 35 percent of the theoretical maximum to reach 80,000 fps (with 5.5 million volts accelerating voltage).

One very promising new technique, applicable to particles of 1/100-gram mass, is the use of a high-energy electrical discharge to vaporize a metal wire or foil. Over 80,000 joules of electrical energy can be stored in a condenser bank and rapidly discharged through the metal foil in a period of microseconds. The energy vaporizes the metal foil, and the vapor is then heated to a temperature which can approach a million degrees Kelvin; the velocity of sound in this gas is very high. It has been reported that the gas has been used to accelerate particles to velocities exceeding 50,000 fps and that even higher velocities are probably attainable.

Semi-infinite target penetration.- In recent years a number of workers have fired numerous projectiles with various combinations of projectile-target materials. The measurements of the crater dimensions, penetration, diameter, and

volume are in most cases correlated by either empirical or semiempirical expressions, or on the basis of nondimensional parameters predicted from dimensional analysis. The difficulty of this latter approach, of course, lies in choosing the appropriate material properties to be used. Usually elastic constants are chosen. A list of some of these empirical expressions is given in table IV and their wide variety reflects the data scatter. Cross correlation between the data from different experiments is sometimes complicated by the fact that portions of the projectile remain at the bottom of the crater. Although some experimenters have measured the depth of penetration as the distance between the original undisturbed surface of the target and the bottom of the actual crater (for example, by sectioning the target), other experimenters have measured the distance between the original undisturbed surface and the top of the projectile in the hole.

Some of the equations listed in table IV are plotted in figure 7. Also shown in the figure are the theoretical results of Bjork (ref. 65). It should be remembered that the experimental data from which the empirical formulas have been developed were obtained at velocities below 30,000 fps, and that the curves in figure 7 have been extrapolated into the meteoroid range. Although there is some agreement at velocities below 30,000 fps, in the meteoroid-velocity range the curves diverge. The theoretical predictions of Bjork, which are based on conditions which would be expected to exist in the meteoroid range, lead to a lesser amount of target damage.

The penetration of semi-infinite targets by metal rods has received relatively little attention. Summers and Niehaus (ref. 66) analyzed experimental results in which the rods suffered only moderate deformation, similar to that of spheres and small cylinders, and concluded that the phenomenon was similar. Slattery and Clay's (ref. 67) firings indicate that rod impact into aluminum for a given velocity is critically dependent upon the mass of the rod and the speed of sound in the rod material. The shape of the crater was conical for impact velocities below the speed of sound, and cylindrical for supersonic impact velocities. A more extensive work was carried out by Allen and Rogers (ref. 68). They reported on the firings of silver, lead, copper, tin, aluminum, and magnesium rods into 7075-T6 aluminum at velocities of from 2,000 to 9,000 fps. Both groups (refs. 67 and 68) observed that the penetration depth was independent of the obliquity of the target. However, the maximum penetration is critically dependent upon the velocity vector being alined with the axis of the rod.

A recent experimental study of projectile penetration into nonmetallic targets (ref. 64) over the range from 500 fps to 20,000 fps indicates that the depth of penetration in nonmetal targets is governed by the same basic parameters as those which apply to metal targets, but the physical nature of the craters differs considerably, being slender and partially filled for the nonmetal targets.

Multiple sheet penetration.- Whipple has suggested that a thin shield, external to and separated from the structure will shatter the approaching meteoroid and thus spread the impact energy over a larger area of the structure. This idea has motivated experiments concerned with the penetration of thin targets. (See table V and ref. 62.) Two sets of data on the effect of bumpers have been published recently: Humes, Hopko, and Kinard (ref. 69) and Funkhauser (ref. 70) investigated the effects of bumper thickness and standoff distance with

copper projectiles at various velocities, and Nysmith and Summers (ref. 71) investigated the effects of a filler material on the minimum velocity required for glass spheres to penetrate a double-sheet structure. (Glass spheres were considered to be representative of frangible meteoroids which shatter easily upon impact.)

Some results of Humes, Hopko, and Kinard's experiments are shown in figure 8, where the total penetration (the sum of the bumper thickness and the depth of the deepest hole in the semi-infinite target) are plotted against the bumper standoff distance with the copper-projectile velocity as a parameter. The bumper was half as thick as the projectile diameter, which was near the optimum thickness. At speeds up to 9,000 fps the projectile pierced the bumper as an unbroken body. At higher velocities the projectile was shattered, and the fragment size decreased as the velocity increased, thus decreasing the depth of the fragment-caused holes in the semi-infinite rear target, provided that the standoff distance was sufficient to permit the fragments to scatter and not more than one impinged at the same point. Thus the amount of damage was directly related to the size of the fragments. The decrease in total penetration was observed as the velocity increased from 9,000 fps to the maximum test velocity of 14,000 fps.

For impact velocities greater than 20,000 fps, Nysmith and Summers (ref. 72) observed that a plate behind a bumper fails in a different manner than for lower speed impact. Some of their data are reproduced in figure 9. At the highest test velocities the projectile and material removed from the bumper are shattered into a thin shell of fine fragments which travel in a diverging pattern. This spray ruptures or cracks the plate behind the bumper before it is perforated by any fragments. Tests at impact velocities of 20,000 fps indicated no change in the ballistic limit when the relative thickness of the bumper and the rear sheet was changed if the sum of their thicknesses was held constant. Going to the extreme of a 1-mil bumper, however, resulted in a great loss in performance because the projectile was not shattered. Nysmith and Summers conclude that, for impact at meteoric speed, a sheet behind a bumper is more likely to be ruptured by a spray of fine particles than to be penetrated by individual particles.

Both sets of experiments demonstrated that for high-velocity impact, the amount of damage is less in a bumper-protected target than in an unprotected target. Additional benefits were derived by placing certain filler materials (glass wool) between the bumper and the target. Care should be used in bumper design to insure that the standoff distance and structural characteristics do not impede the bumper mechanism; i.e., the particles and blast pressure must be allowed to expand.

Current effort.- Table V is a list of current impact studies.

PROTECTION METHODS

Types of Structural Damage

The end result of structural damage under meteoritic impact may vary widely in kind, and different measures of protection may be necessary:

(1) Simple leakage - significant for cabins, propellant tanks, radiators, and inflatable structure

(2) Explosive perforation - perforation of structure under tensile stress, such as a pressure vessel, permitting unstable release of strain energy, rapid crack propagation, and catastrophic failure

(3) Explosive intrusion - energy of incident particle transmitted to internally contained fluid, creating high-energy shock waves which cause extensive damage to container structure at local or distant points

(4) Partial surface damage - cratering resulting in structural weakness which may constitute a latent source of failure

(5) Damage to function - introducing deformation or contamination which would interfere with proper operation of equipment or mechanism. Erosion or surface pitting which would change the surface heat adsorbtivity or reflectivity

(6) Ignition - creation of local temperature and pressure conditions which may cause ignition of propellants or initiate chemical action in materials. There is a hazard of local flash burns to nearby personnel (ref. 73)

(7) Chipping - pocking of heat shield which may cause malfunction during reentry

(8) Spalling - introduction of high-velocity particles from the back side of target sheet without complete penetration, creating a hazard to men and equipment in cabins

Application of Meteoroid Flux Data and Impact Data to Design Problems

The question of how thick the vehicle hull or structure must be made in order to assure a sufficiently low probability of sustaining damage resulting from meteoroid impact involves the statistical problem of the likelihood of meteoroid encounter during the mission, and this depends upon the environment, the duration and path of the flight, and the size of the vehicle or component under consideration. The damage phenomenon might also be treated in a statistical fashion. Various estimates have been made of the hazard in references 65, 71, 73, 74, and 75.

The treatment of the problem depends upon the present quantitative knowledge of the meteoroid environment and the effects of high-speed impact, neither of which is defined with anything like comfortable certainty. The natural engineering tendency to bracket the problem by designing for the most pessimistic outlook leads, in some cases, to such an intolerable weight of protective devices that the feasibility of the mission becomes questionable.

Demonstrative calculations have been made herein to show how the estimates of the probability of meteoroid puncture are made. A statistical approach is used because a collision between a meteoroid and a vehicle depends upon chance. For the purpose of illustration herein, three calculations have been made; the input data are such that the estimates of the severity of the hazard range from pessimistic to optimistic. These three cases are: (1) Whipple's (1961) estimate of the meteoroid flux and a single-sheet aluminum skin; (2) Watson's estimate of the meteoroid flux and a single-sheet aluminum skin; and (3) Whipple's (1961) estimate of the meteoroid flux and velocities and an aluminum bumper shield. For the unprotected structures Bjork's penetration equation will be used (which, because Bjork's calculations are restricted to a projectile and target of the same material, somewhat conservatively considers the density of the meteoroid to be 2.7 g/cm^3). Experiments have shown that a projectile will just penetrate a thin sheet which is 1.5 times as thick as the penetration depth in a semi-infinite target (ref. 62), so the semi-infinite target penetration equations can be used to calculate the sheet thickness if the results are multiplied by 1.5. For the bumper-shielded structures, the preliminary results of reference 72 will be used. All calculations will be for a vehicle with 750 square feet of surface area which must spend 14 days in space with a 0.99 probability of not having a puncture or rupture of the main cabin wall.

For a random distribution of meteoroids, where the most probable number of penetrations ϵ is much smaller than the extremely large number of meteoroids in space, the probability of having exactly r penetrations in a given flight is

$$P_{(r)} = \frac{\epsilon^r}{r!} e^{-\epsilon}$$

if ϵ is a constant. As has been done in all calculations in the past, it will be assumed here that ϵ is a constant, even though (as has been mentioned previously) it is known that the meteoroid flux varies from day to day (even if severe visible meteor showers are not considered). There are little statistical data on the severity of these flux fluctuations; it is assumed that over a "sufficiently long" period the vehicle will effectively encounter the average flux. The effect of the actual variations will tend to increase the standard deviation of the probability of puncture to a value which is greater than that for a constant flux condition. The use of this procedure herein is justified only on the basis that there is insufficient knowledgeable data on flux variations to permit a rational analysis of their effect.

It is sometimes of interest to know the probability that the number of penetrations will not exceed some number K. The probability that the number of penetrations will be K or less is

$$p(r \leqq K) = e^{-\epsilon} \frac{\epsilon^0}{0!} + e^{-\epsilon} \frac{\epsilon}{1!} + e^{-\epsilon} \frac{\epsilon^2}{2!} + \cdots + e^{-\epsilon} \frac{\epsilon^K}{K!}$$

$$= e^{-\epsilon} \sum_{n=0}^{K} \frac{\epsilon^n}{n!}$$

Reference 76 contains tables which are useful in evaluating Poissonian probabilities.

At present the conditions of interest are those under which the probability of receiving zero punctures is 0.99, or

$$0.99 = \frac{\epsilon^0}{0!} e^{-\epsilon}$$

from which

$$\epsilon = -\log_e 0.99 = 0.01005$$

Thus, the most probable number of penetrations must be equal to or less than 0.01005. For a 14-day mission with 750 square feet of surface area, the penetration rate cannot exceed

$$\psi = \frac{\epsilon}{A\tau} = \frac{0.01005}{750 \times 14} = 9.58 \times 10^{-7} \qquad \frac{\text{penetrations}}{\text{ft}^2\text{-day}}$$

An approximation to Bjork's penetration results for aluminum on aluminum impact is

$$P = 1.09(mV)^{1/3} \qquad \text{centimeters}$$

for the depth of penetration in semi-infinite targets. For the thickness of a sheet which will just stop penetration, this becomes

$$t = \frac{1.5(1.09)}{2.54}(mV)^{1/3} \qquad \text{inches}$$

where m is in grams and V is in km/sec. Table II with column 2 divided by 10 to get the so-called 1961 estimate and column 4, as it stands supplies the required input data from which, with column 8, the penetration flux as a function of aluminum skin thickness can be calculated. The results of the calculations are

shown in figure 10. For a penetration rate of 9.58×10^{-7} penetration ft^{-2}-day^{-1}, the necessary skin thickness is 0.16 inch. More conservative results (and a thicker skin) would have been obtained if Whipple's 1957 table and Charters and Summers' penetration equation had been used.

On the optimistic side, if Watson's curve in figure 10 is used, a thickness of 0.025 inch is obtained. It is obvious from this calculation that meteoroids present no problem to some vehicles if the design criterion be restricted to puncture and structural weakening is not considered, because aluminum thicknesses of this amount probably might be used for reasons of structural strength and/or stiffness.

An estimate of the effectiveness of a bumper design can be made by comparing the results of Nysmith and Summers thin-sheet penetration experiments with Charters and Summers' semi-infinite target-penetration equation modified to apply to thin (unprotected) sheets. From figure 9 an approximate analytical expression in the upper range of velocity might be

$$t/d = 0.287\ V^{2/3}$$

where V is in km/sec. If a spherical projectile is assumed, the total thickness of a double-sheet structure with a sheet separation of 8 diameters and with each sheet the same thickness becomes

$$t_b = 0.356\left(\frac{1}{\rho_p}\right)^{1/3}\left(mV^2\right)^{1/3}$$

Charters and Summers' equation for the depth of penetration in a semi-infinite target is (ref. 52)

$$\frac{P}{d} = 2.28\left(\frac{\rho_p}{\rho_t}\right)^{2/3}\left(\frac{V}{c}\right)^{2/3}$$

where c is the velocity of sound in the target material. Kinard et al. (ref. 62) have shown that, under given conditions of projectile velocity, mass, etc., if the projectile will make a crater P centimeters deep in a semi-infinite target, the same projectile under the same conditions could make a hole through a thin-sheet target

$$t_1 = 1.5P$$

centimeters thick, where t_1 is the thickness of a single sheet. It will be assumed that Charters and Summers' equation can be multiplied by 1.5 to obtain the thickness of a thin sheet which will be penetrated. Thus

$$\frac{t_1}{d} = (1.5)(2.28)\left(\frac{\rho_p}{\rho_t}\right)^{2/3}\left(\frac{V}{c}\right)^{2/3}$$

Again assuming a spherical projectile, and also assuming an aluminum target in which $\rho_t = 2.7$ g/cm^3 and $c = 5.1$ km/sec

$$t_1 = 0.736\left(\rho_p\right)^{1/3}\left(mV^2\right)^{1/3} \qquad \text{centimeters}$$

The ratio between t_b and t_1 is

$$\frac{t_b}{t_1} = \frac{0.356}{0.736}\left(\frac{1}{\rho_p}\right)^{2/3} = 0.48\left(\frac{1}{\rho_p}\right)^{2/3}$$

which shows that the bumper becomes more effective as the density of the projectile increases. In order to compare the bumper effectiveness with the previous calculations, a meteoroid density of 2.7 g/cm^3 will be assumed. Then

$$\frac{t_b}{t_1} = 0.25$$

or, the total structure weight is diminished by a factor of four. Further improvement might be obtained by increasing the standoff distance. On the other hand, if similar manipulations be performed with Bjork's penetration equation, the benefits derived from a bumper design might not be as great; Bjork's equation predicts less damage in an unprotected target than does that of Charters and Summers.

This calculation illustrates that bumper designs can be useful in reducing the weight necessary to protect space vehicles from meteoroid puncture. Further experiments may help in arriving at more efficient bumper designs. These calculations were made only for purposes of illustration; other assumptions which might be used in computing the relative thicknesses between the double-sheet structure and the single-sheet structure might lead to different quantitative estimates of the bumper efficiency.

It is likely that the interior cabin walls of manned space vehicles will be inaccessible because they will be covered with equipment necessary to operate the vehicle, and, therefore, it may be impossible to repair punctures from the interior of the vehicle. Many of the components which are responsible for the safety of the crew of a manned vehicle have been specified to have a minimum reliability of 0.999, in order that the overall reliability of the equipment which consists of many components shall approach 0.99. If a meteoroid penetration be considered a threat to crew safety, particularly if there be little hope of effecting a repair, then it follows that a vehicle should be designed for a

probability of 0.999 of not having a meteoroid puncture. This is a vehicle which is 10 times more reliable than those considered previously. For the purposes of comparison, the same vehicle area and flight period will be used here as was used in the preceding examples. Also, a very conservative "bracketing" engineering estimate will be used to establish an upper limit on the amount of required protection. Again, however, the variations in flux rate will be ignored for the same reasons that were stated previously.

The most conservative estimate of the frequency-mass distribution - that of Whipple (1957) - will be used in conjunction with the penetration estimate of Charters and Summers. Although Charters and Summers' equation is not the most conservative (see fig. 7), the combination with Whipple's (1957) estimate is considered conservative, particularly in light of the results obtained from the two-day flight of Explorer XIII.

The most probable number of punctures cannot exceed

$$\epsilon = -\log_e 0.999 = 0.001$$

As before, a single-thickness aluminum skin will be assumed. However, in order to be consistent with the attempt to obtain a conservative estimate of the penetration flux, it might be logical to assume a meteoroid density of 3.5 g/cm^3 (approximately that of stone) instead of the previously assumed value of 2.7 g/cm^3. Such a value of density would lead to only a 12-percent increase in sheet thickness; this increase is small compared with the possible order of magnitude variations in mass-flux estimates. Therefore, in order to compare the results of this calculation with the previously calculated skin thickness, the value of 2.7 g/cm^3 will be assumed here also. On this basis, then, Charters and Summers' equation becomes, after a conversion to inches

$$t = 0.404\left(mV^2\right)^{1/3} \qquad \text{inches}$$

For a most probable number of penetrations of 0.001, the allowable penetration flux is

$$\Psi = \frac{0.001}{150 \times 4} = 4.76 \times 10^{-7} \qquad \frac{\text{penetrations}}{ft^2\text{-day}}$$

which, from figure 10, indicates a required skin thickness of 1.0 inch.

Part of the reason for the marked increase in the meteoroid-protection weight computed here and that computed in the previous section is that the vehicle just considered is 10 times more reliable. Another reason is the use of a more conservative penetration equation. For the purpose of direct comparison, to illustrate the effect of the conservative flux and penetration equations this last case can be calculated for a vehicle which is 0.990 reliable. The single-skin thickness

would then be 0.5 inch. (As a rough rule of thumb, an order of magnitude decrease in reliability reduces the total skin weight by a factor of one-half.)

This last set of calculations, however, illustrates the magnitude of the designer's dilemma if he attempts to employ the standard methods of conservative engineering design to the meteoroid problem.

RESEARCH IN PROGRESS

Ground Research

Facilities.- Table VI lists facilities available for ground tests. Accelerating devices are under continual improvement. Improvements are being made in radar detection systems. Luminous efficiency experiments are continuing and hopefully will supply calibration data to relate meteors and meteoroid masses.

Projects underway.- Table V is a brief description of some of the projects in progress or proposed. Proposed projects are mentioned only as illustrations of current thinking. Some studies of hypervelocity impact into very thick targets is continuing in an effort to discover the physical laws governing penetration. Experimental programs have been started to evaluate the effectiveness of bumper shields because use of shields shows promise as a means of decreasing the meteoroid damage to space vehicles with only a modest increase in the weight of the structure. Light-gas guns are being used to evaluate comparatively the susceptibility to damage of materials such as metals, plastics, and ceramics which may be exposed to meteoroids. Exploding metal-foil accelerators are being improved.

Flight Test Research

Space vehicles in orbit.- No space vehicles are presently transmitting meteoroid information (April 1962).

Proposed flight tests.- The S-55B is scheduled for launch in 1962. Table VII is a partial list of proposed flight experiments, mainly by the NASA Goddard Space Flight Center.

RECOMMENDED METEOROID RESEARCH PROGRAM

Consideration of the compiled data in the previous sections of this report shows that, while a great deal of information regarding meteoroids has been collected, application of this information to an engineering design may involve so much inaccuracy that merely to cover the range of uncertainty introduces a gross and intolerable weight penalty. The most important research task at the moment is to narrow substantially the current uncertainty in penetration rates for various materials, as is illustrated in figure 10.

The objectives that have been selected as suitable for a research attack on the meteoroid damage problem are (a) to determine whether meteoroids constitute an important hazard to spacecraft, and if so (b) to provide the designer with the information that he needs to protect the spacecraft against this hazard. To illustrate the relationships and interdependence among the many items of research that contribute to the overall knowledge, a flow chart has been prepared and is shown in figure 11. Major items that might provide necessary or useful information have in some cases been included even though they do not appear entirely feasible at present; on the other hand, in the interest of clarity, specific details related to particular experiments are not shown.

At the right of the chart is a box labeled "damage statistics for the design of space vehicles." This represents the objective. Two approaches to this objective are evident in the chart; each path has its own particular advantages and disadvantages, and neither by itself will supply sufficient information to solve the meteoroid problem. In general, the two paths are:

(a) A direct approach which utilizes satellites and probes to determine directly penetration-damage statistics.

(b) An indirect approach which utilizes satellites and probes, radar observation, photographic observation, and radio observation to obtain data on the flux, mass, velocity, orbital parameter, and density of meteoroids. These data would be used in the design of ground impact tests which would yield the desired damage information for design purposes.

It should not be assumed that the necessity for a choice between two alternatives is implied. On the contrary, the two approaches are complementary, rather than mutually exclusive. Experience has shown that a balanced research program produces the greatest benefits with the least cost.

The direct approach to the evaluation of the damage statistics consists of flight experiments designed so that structural materials will be punctured or damaged. The number of punctures and/or the extent of the damage are telemetered to ground stations. The advantage of this approach is that the data are immediately available for the subsequent design of space vehicles. Because payload weight is limited by the boosters available, it is impractical to measure reliability by launching a replica of a specific vehicle. Such a manner of testing is prohibited by the large area-time ratio of the test vehicle to the actual vehicle required to infer high statistical confidence in the results. This difficulty may possibly be circumvented by utilizing several thicknesses of somewhat thinner material than would be used in actual structures, and defining experimentally the variation in penetration damage as a function of thickness. But this approach will require extrapolation of the results to actual structural thicknesses. The size limitation also restricts the number of penetrations which can be expected, and complete information about meteoroid temporal flux variations, therefore, is better obtained by the indirect approach.

The indirect approach provides a detailed picture of the meteoroid phenomenon and the mechanisms of hypervelocity impact. The primary means of obtaining meteoroid flux data are those enclosed within the dotted boundaries in the flow diagram. Two important requirements exist here, in that (1) calibration of and

correlation among the various methods must be performed (these experiments are indicated to the left of the dashed boundaries), and (2) that ground-facility capabilities must be improved to obtain sufficiently high velocities to provide good simulation of meteoroid damage. The methods which are to be coordinated in the indirect approach are:

(a) Satellites and probes which carry sensors that measure various meteoroid characteristics. These sensors can measure impact events, or flux distributions, meteoroid velocity, crater size, light flash, energy, momentum, etc.

(b) Photographic and radar observation of the sky. As indicated in the flow chart, these methods require determination of the relationship between the photographic brightness, or radar ionization reflectivity, and the mass of the meteoroid. These relationships can be determined by means of the procedures and experiments shown on the left of the flow chart. The recoverable flight experiments will provide micrometeoroid material for physical and chemical examination.

(c)* Radio observation of the sky. The scattering of radio signals by reflection and refraction from the ionization trails formed by meteoroids entering the Earth's atmosphere has been under observation for many years. Probably very little information about the physical characteristics of meteoroids is obtainable from these data. The method does offer the advantage of obtaining temporal flux variations in the upper atmosphere with inexpensive unattended equipment.

(d) Laboratory penetration tests. After the characteristics of meteoroid particles are determined, it is necessary to determine the damage that will be done by a particle of a given size, mass, and velocity to space-vehicle structures. The required information should be determined by tests in ground-based hypervelocity ballistic ranges.

The indirect approach by itself is a long and tedious process. The inaccuracy of the results is essentially the sum of the inaccuracies in the several component experiments shown in the flow chart. The significance of this point is illustrated by the very poor accuracy of the present information on meteoroid damage, which has been obtained by the indirect approach. On the other hand, the indirect approach can provide important contributions, for example, a more complete picture of the meteoroid population and characteristics, and of the impact and penetration mechanisms. Furthermore, the area of sky that can be observed from the Earth is so much larger than the area of any object that can be put into orbit, that the potential area-time exposure for ground-based observations is orders of magnitude greater than for orbital experiments. A tremendous amount of information can be gleaned even from past photographs and radar observations as soon as accurate mass-brightness and mass-reflectivity calibrations are obtained.

To summarize, the direct approach offers better accuracy at the present, but is limited in the amount of information it can provide. The indirect approach is inaccurate now, but is capable of supplying a large amount of information in the future. The accuracy of the indirect approach can be improved, but this requires a long-range research effort. A certain amount of direct experimentation would be necessary even if the accuracy of the indirect approach was thought to be

satisfactory in order to confirm the empirical or theoretical relations. Thus, these two approaches are complementary. The research program should include both and they should be kept in proper balance in order to minimize total cost and to afford the most rapid advance in accuracy. Considering the gross national effort, it is apparent that such a necessary balance does not exist at present. Only one experimental program of the direct structural penetration type (the NASA S-55 satellite) has been established. The committee expressly recommends an increase in effort toward the direct flight measurement of structural penetration and damage, and that support should be given to the improvement of the capabilities and data gathering accuracies of the ground-based facilities.

Langley Research Center,
National Aeronautics and Space Administration,
Langley Station, Hampton, Va., September 24, 1962.

REFERENCES

1. Grimminger, G.: Probability That a Meteorite Will Hit or Penetrate a Body Situated in the Vicinity of the Earth. Jour. Appl. Phys., vol. 19, no. 10, Oct. 1948, pp. 947-956.

2. Whipple, Fred L.: The Meteoritic Risk to Space Vehicles. Vol. I of Vistas in Astronautics, Morton Alperin and Marvin Stern, eds., Pergamon Press (New York), c.1958, pp. 115-124.

3. Lovell, A. C. B.: Geophysical Aspects of Meteors. Encyclopedia of Phys., vol. XLVIII, Geophysics II, Springer - Verlag (Berlin), 1957, pp. 427-454.

4. Whipple, Fred L.: A Comet Model. III. The Zodiacal Light. The Astrophysical Jour., vol. 121, no. 3, May 1955, pp. 750-770.

5. Whipple, Fred L., and Hawkins, Gerald S.: Meteors. Encyclopedia of Phys., vol. LII, Astrophysics III: The Solar System, Springer - Verlag (Berlin), 1959, pp. 519-564.

6. Whipple, Fred L.: The Theory of Micro-Meteorites. Part I. In an Isothermal Atmosphere. Proc. Nat. Acad. Sci., vol. 36, no. 12, Dec. 1950, pp. 687-695.

7. Whipple, Fred L.: The Theory of Micro-Meteorites. Part II. In Heterothermal Atmospheres. Proc. Nat. Acad. Sci., vol. 37, no. 1, Jan. 1951, pp. 19-30.

8. Dubin, Maurice, and McCracken, Curtis W.: Measurements of Distributions of Interplanetary Dust. The Astronomical Jour., vol. 67, no. 5, June 1962, pp. 248-256.

9. Alexander, W. M., McCracken, C. W., Secretan, L., and Berg, O. E.: Review of Direct Measurements of Interplanetary Dust From Satellites and Probes. A paper presented at the COSPAR Meeting May 1962. (To be published in Proc. Third Int. Space Sci. Symposium by North Holland Pub. Co.)

10. Herrmann, Walter, and Jones, Arfon H.: Survey of Hypervelocity Impact Information. A.S.R.L. Rep. No. 99-1 (Contract AF 19 (604)-7400), M.I.T., Sept. 1961; Addendum, Oct. 1961.

11. Davison, Elmer H., and Winslow, Paul C., Jr.: Space Debris Hazard Evaluation. NASA TN D-1105, 1961.

12. Robey, Donald H.: Meteoritic Dust and Ground Simulation of Impact on Space Vehicles. Jour. British Interplanetary Soc., vol. 17, no. 1, Jan.-Feb. 1959, pp. 21-30.

13. Jacchia, Luigi G.: The Physical Theory of Meteors. VIII. Fragementation as Cause of the Faint-Meteor Anomaly. The Astrophysical Jour., vol. 121, no. 2, Mar. 1955, pp. 521-527.

14. Gallagher, P. B., and Eshelman, V. R.: 'Sporadic Shower' Properties of Very Small Meteors. Jour. Geophys. Res., vol. 65, no. 6, June 1960, pp. 1846-1847.

15. Goettelman, R. C., Softky, S. D., Arnold, J. S., and Farrand, W. B.: The Meteoroid and Cosmic-Ray Environment of Space Vehicles and Techniques for Measuring Parameters Affecting Them. WADD Tech. Rep. TR 60-846 (Contract No. AF 33(616)-7015), U.S. Air Force, Dec. 1960.

16. Barnes, Virgil E.: Tektites. Scientific American, vol. 205, no. 5, Nov. 1961, pp. 58-65.

17. Chapman, Dean R., Larson, Howard K., and Anderson, Lewis A.: Aerodynamic Evidence Pertaining to the Entry of Tektites Into the Earth's Atmosphere. NASA TR R-134, 1962.

18. Watson, Fletcher G.: Between the Planets. Rev. ed., Harvard Univ. Press (Cambridge, Mass.), 1956.

19. Payne-Gaposchkin, Cecilia: Introduction to Astronomy. Prentice-Hall, Inc., 1954.

20. Wyatt, Stanley P., Jr., and Whipple, Fred L.: The Poynting-Robertson Effect on Meteor Orbits. The Astrophysical Jour., vol. 111, Jan. 1950, pp. 134-141.

21. Hawkins, Gerald S., and Southworth, Richard B.: The Statistics of Meteors in the Earth's Atmosphere. Smithsonian Contributions to Astrophysics, vol. 2, no. 11, 1958.

22. McCrosky, Richard E.: Observations of Simulated Meteors. Smithsonian Contributions to Astrophysics, vol. 5, no. 4, 1961.

23. Whipple, Fred L.: Particulate Contents of Space. Medical and Biological Aspects of the Energies of Space, Paul A. Campbell, ed., Columbia Univ. Press (New York), 1961, pp. 49-70.

24. Öpik, Ernst J.: Physics of Meteor Flight in the Atmosphere. Interscience Pub., Inc. (New York), 1958.

25. Öpik, E. J.: Interplanetary Dust and Terrestrial Accretion of Meteoric Matter. Irish Astronomical Jour., vol. 4, 1956, pp. 84-135.

26. LaGow, H. E., and Alexander, W. M.: Recent Direct Measurements by Satellites of Cosmic Dust in the Vicinity of the Earth. NASA TN D-488, 1960.

27. McCracken, C. W., Alexander, W. M., and Dubin, M.: Direct Measurements of Interplanetary Dust Particles in the Vicinity of Earth. NASA TN D-1174, 1961.

28. Alexander, W. M., McCracken, C. W., and LaGow, H. E.: Interplanetary Dust Particles of Micron Size Probably Associated With the Leonid Meteor Stream. NASA TN D-1154, 1961.

29. Soberman, R. K., and Lucca, L. Della: Micrometeorite Measurements From the Midas II Satellite (1960 ζ1). GRD Res. Notes No. 72 (AFCRL 1053), Air Force Cambridge Res. Labs., Nov. 1961.

30. Duberg, John E.: The Meteoric Hazard of the Environment of a Satellite. NASA TN D-1248, 1962.

31. Whipple, Fred L.: The Dust Cloud About the Earth. Nature, vol. 189, no. 4759, Jan. 14, 1961, pp. 127-128.

32. Soberman R. K., ed.: Micrometeorite Collection From a Recoverable Sounding Rocket. GRD Res. Notes No. 71 (AFCRL 1049), Air Force Cambridge Res. Labs., Nov. 1961.

33. Nazarova, T. N.: Rocket and Satellite Meteoric Dust Investigations. Twelfth Int. Astronautical Congress (Washington, D.C.), Oct. 1-7, 1961.

34. Nazarova, T. N.: The Results of Studies of Meteoric Dust by Means of Sputnik III and Space Rockets. Space Research, Hilde Kallmann Bijl, ed., Interscience Publ., Inc. (New York), 1960, pp. 1059-1062.

35. Anon.: How Satellite Measures Micrometeoroids. Electronics, vol. 34, no. 34, Aug. 25, 1961, p. 24.

36. Zaid, Melvin, and Paul, Burton: Armor Penetration. Ordnance, vol. 4, no. 220, Jan.-Feb., 1957, pp. 609-611.

37. Bethe, H. A.: Attempt of a Theory of Armor Penetration. Ordnance Lab., Frankford Arsenal (Philadelphia), May 23, 1941.

38. Taylor, G. I.: The Formation and Enlargement of a Circular Hole in a Thin Plastic Sheet. Quarterly Jour. Mech. and Appl. Math., vol. 1, pt. 1, March 1948, pp. 103-124.

39. Thomson, William T.: An Approximate Theory of Armor Penetration. Jour. Appl. Phys., vol. 26, no. 1, Jan. 1955, pp. 80-82; Note on "An Approximate Theory of Armor Penetration." Jour. Appl. Phys. (Letters to the Editor), vol. 26, no. 7, July 1955, pp. 919-920.

40. Zaid, Melvin, and Paul, Burton: Mechanics of High Speed Projectile Perforation. Jour. Franklin Inst., vol. 264, no. 1, July 1957, pp. 117-126.

41. Zaid, Melvin, and Paul, Burton: Normal Perforation of a Thin Plate by Truncated Projectiles. Jour. Franklin Inst., vol. 265, no. 4, Apr. 1958, pp. 317-335.

42. Zaid, Melvin, and Paul, Burton: Oblique Performation of a Thin Plate by a Truncated Conical Projectile. Jour. Franklin Inst., vol. 268, no. 1, July 1959, pp. 24-45.

43. Zaid, M.: An Analytical Approach to Hypervelocity Impact Mechanics. Hypervelocity Impact - Fourth Symposium Apr. 26, 27, 28, 1960. APGC-TR-60-39 (III), U.S. Air Force, Sept. 1960. (Available from ASTIA as AD 244 477.)

44. Birkhoff, Garrett, MacDougall, Duncan P., Pugh, Emerson M., and Taylor, Geoffery: Explosives With Lined Cavities. Jour. Appl. Phys., vol. 19, no. 6, June 1948, pp. 563-582.

45. Pack, D. C., and Evans, W. M.: Penetration by High-Velocity ("Munroe") Jets: I. Proc. Phys. Soc. (London), vol. 64, pt. B, no. 376B, Apr. 1, 1951, pp. 298-302.

46. Cook, M. A.: Mechanism of Cratering in Ultra-High Velocity Impact. AFOSR TN 57-486, U.S. Air Force, July 10, 1957.

47. Rostoker, Norman: The Formation of Craters by High-Speed Particles. Meteoritics. vol. 1, no. 1, 1953, pp. 11-27.

48. Öpik, Ernst: Researches on the Physical Theory of Meteor Phenomena. I. Theory of the Formation of Meteor Craters. T.P. 28, Acta et Comm. Univ. Tartuensis, 1936.

49. Bjork, R. L.: Numerical Solutions of the Axially Symmetric Hypervelocity Impact Process Involving Iron. Proc. Third Symposium on Hypervelocity Impact. vol. II, Armour Res. Foundation, Illinois Inst. Tech., Feb. 1959, pp. 35-65.

50. Langton, N. H.: The Thermal Dissipation of Meteorites by Bumper Screens. Bericht über den V. Internationalen Astronautischen Kongress (Insbruck), Friedrich Hecht, ed., 1955, pp. 72-80.

51. McDermott, C. E., Cannon, E. T., and Grow, R. W.: Temperature Studies and Effects in Perforation of Thin Aluminum Targets. Tech. Rep. UU-3, Univ. of Utah, May 1959.

52. Lavrent'yev, M. A.: The Problem of Piercing at Cosmic Velocities. NASA TT F-40, 1960.

53. Rinehart, John S., and Pearson, John: Behavior of Metals Under Impulsive Loads. American Soc. for Metals, Cleveland, 1954.

54. Stanyukovich, K. P.: Concerning the Impact of Solids at High Velocities. Soviet Physics - JETP (Letters to the Editor), vol. 36(9), no. 5, Nov. 1959, p. 1141.

55. Kineke, John H., Jr.: An Experimental Study of Crater Formation in Metallic Targets. Hypervelocity Impact - Fourth Symposium Apr. 26, 27, 28, 1960. APGC-TR-60-39(I), U.S. Air Force, Sept. 1960. (Available from ASTIA AS AD 244475.)

56. Genevese, F., ed.: Proc. Third Symposium on Hypervelocity Impact, vol. 1, Armour Res. Foundation, Illinois Inst. Tech., Feb. 1959.

57. Huth, J. H., Thompson, J. S., and Van Valkenburg, M. E.: Some New Data on High-Speed Phenomena. Jour. Appl. Mech., vol. 24, no. 1, Mar. 1957, pp. 65-68.

58. Kinard, William H., and Collins, Rufus D., Jr.: A Technique for Obtaining Hypervelocity Impact Data by Using the Relative Velocities of Two Projectiles. NASA TN D-724, 1961.

59. Anon.: Hypervelocity Impact - Fourth Symposium Apr. 26, 27, 28, 1960. APGC-TR-60-39(III), U.S. Air Force, Sept. 1960. (Available from ASTIA as AD 244 477.)

60. Charters, A. C., and Summers, James L.: Comments on Phenomena of High-Speed Impact. Addresses at the Dedication of the New NOL Aeroballistic Research Facilities and at the Decennial Symposium on Aeroballistics. NOLR 1238, U.S. Naval Ord. Lab. (White Oak, Md.), Oct. 1960, pp. 200-221.

61. Summers, James L.: Investigation of High-Speed Impact: Regions of Impact and Impact at Oblique Angles. NASA TN D-94, 1959.

62. Kinard, William H., Lambert, C. H., Schryer, David R., and Casey, Francis W., Jr.: Effect of Target Thickness on Cratering and Penetration of Projectiles Impacting at Velocities to 13,000 Feet Per Second. NASA MEMO 10-18-58L, 1958.

63. Collins, Rufus D., Jr., and Kinard, William H.: The Dependency of Penetration on the Momentum Per Unit Area of the Impacting Projectile and the Resistance of Materials to Penetration. NASA TN D-238, 1960.

64. Kinard, William H., and Collins, Rufus D., Jr.: An Investigation of High-Velocity Impact Cratering Into Nonmetallic Targets and Correlation of Penetration Data for Metallic and Nonmetallic Targets. NASA TN D-726, 1961.

65. Bjork, Robert L.: Meteoroids Versus Space Vehicles. [Preprint] 1200-60, American Rocket Soc., May 1960.

66. Summers, James L., and Niehaus, William R.: A Preliminary Investigation of the Penetration of Slender Metal Rods in Thick Metal Targets. NASA TN D-137, 1959.

67. Slattery, R. E., and Clay, W. G.: The Penetration of Thin Rods Into Aluminum. Hypervelocity Impact - Fourth Symposium Apr. 26, 27, 28, 1960. APGC-TR-60-39 (III), U.S. Air Force, Sept. 1960. (Available from ASTIA as AD 244 477.)

68. Allen, William A., and Rogers, James W.: Penetration Into a Thick Aluminum Target. NAVWEPS REP. 7597, NOTS TP 2687, U. S. Naval Ord. Lab. (China Lake, Calif.), Dec. 1, 1960.

69. Humes, Donald, Hopko, R. N., and Kinard, William H.: An Experimental Investigation of Single Aluminum Meteor Bumpers. Proc. Fifth Symposium on Hypervelocity Impact, vol. 1, pt. 2, Naval Res. Lab. (Washington, D.C.), April 1962, pp. 567-580.

70. Funkhauser, M.: Estimates of the Penetration of the Skin of a Satellite by Meteoroids. Appl. Mech. Memo. no. 50, Missiles and Ordnance Systems Dept., General Electric Co., Apr. 1958.

71. Nysmith, C. Robert, and Summers, James L.: Preliminary Investigation of Impact on Multiple-Sheet Structures and an Evaluation of the Meteoroid Hazard to Space Vehicles. NASA TN D-1039, 1961.

72. Nysmith, C. Robert, and Summers, James L.: An Experimental Investigation of the Impact Resistance of Double-Sheet Structures at Velocities to 24,000 Feet Per Second. NASA TN D-1431, 1962.

73. Thompson, A. B., and Gell, C. F.: Meteoroids as a Hazard in Space Flight - A Survey of Present Information. [Preprint] 2138-61, American Rocket Soc., Oct. 1961.

74. Bjork, Robert L., and Gazley, Carl, Jr.: Estimated Damage to Space Vehicles by Meteoroids. U. S. Air Force Project RAND Res. Memo. RM-2332, The RAND Corp., Feb. 20, 1959.

75. Lampert, S., and Younger, D. G.: Multi-Wall Structures for Space Vehicles. WADD Tech. Rep. 60-503, U.S. Air Force, May 1960.

76. Molina, E. E.: Poisson's Exponential Bionominal Limit. D. Van Nostrand Co., Inc., 1942.

77. Van Valkenburg, M. E., Clay, Wallace G., and Huth, J. H.: Impact Phenomena at High Speeds. Jour. Appl. Phys., vol. 27, no. 10, Oct. 1956, pp. 1123-1129.

78. Pugh, E. M., and Eichelberger, R. J.: Crater Formation in Metals by High-Velocity Fragments. Proc. Rand Symposium on High-Speed Impact. (Santa Monica), Contract No. AF 33(038)-6413, May 1, 1955.

79. Partridge, William S., Van Fleet, Howard B., and Whited, Charles R.: An Investigation of Craters Formed by High-Velocity Pellets. Tech. Rep. No. OSR-9, Dept. Elec. Eng., Univ. of Utah, May 1957.

80. Partridge, William S., and Clay, Wallace G.: Studies of High-Velocity Impact in Wax. Jour. Appl. Phys., vol. 29, no. 6, June 1958, pp. 939-942.

81. Engel, Olive G.: Pits in Metals Caused by Collision With Liquid Drops and Soft Metal Spheres. Res. Paper 2958, Jour. Res. Nat. Bur. Standards, vol. 62, no. 6, June 1959, pp. 229-246.

82. Charters, A. C., and Locke, G. S., Jr.: A Preliminary Investigation of High-Speed Impact: The Penetration of Small Spheres Into Thick Copper Targets. NACA RM A58B26, 1958.

83. Anderson, G. D.: Studies in Hypervelocity Impact. Poulter Lab. Tech. Rep. 018-59, Dec. 1959.

84. Maiden, C. J., Charest, J., and Tardif, H. P.: An Investigation of Spalling and Crater Formation by Hypervelocity Projectiles. Hypervelocity Impact - Fourth Symposium Apr. 26, 27, 28, 1960. APGC-TR-60-39 (III), U.S. Air Force, Sept. 1960. (Available from ASTIA as AD 244 477.)

85. Atkins, W. W., and Swift, H. F.: Hypervelocity Capability and Impact Research. NRL Memo Rep. 1115, Dec. 1960.

86. Hawkins, Gerald S.: A Radio Echo Survey of Sporadic Meteor Radiants. Monthly Notice, Rep. Astronomical Soc., vol. 116, no. 1, 1956, pp. 92-104.

BIBLIOGRAPHY

Edmiston, R. M.: The Production of Meteoroid Hole Area in a Space Vehicle Near the Earth. IAS Paper no. 62-29, Jan. 1962.

Eichelberger, R. J., and Gehring, J. W.: Effects of Meteoroid Impacts on Space Vehicles. [Preprint] 2030-61, American Rocket Soc., Oct. 1961.

Harrington, H. E., and Buck, Richard F.: Acoustic Detection of Meteoric Particles. AFCRC-TR-60-272, Air Force Cambridge Res. Center, 1960.

Hawkins, Gerald S.: The Relation Between Asteroids, Fireballs, and Meteorites. The Astronomical Jour., vol. 64, no. 10, Dec. 1959.

Jaffe, Leonard D., and Rittenhouse, John B.: Behavior of Materials in Space Environments. ARS Jour., vol. 32, no. 3, Mar. 1962, pp. 320-346.

Kornhauser, Maury: Prediction of Cratering by Meteoroid Impacts. Advances in Astronautical Sciences, vol. 2, Plenum Press, Inc., New York, 1958, pp. 33-1 - 33-13.

LaPaz, Lincoln: Meteoroids, Meteorites, and Hyperbolic Meteoritic Velocities. Physics and Medicine of the Upper Atmosphere. Univ. of New Mexico Press (Albuquerque), 1952, pp. 352-393.

Livingston, W. A., and Hart, E. M.: The Effects of Natural Environment in Cis-lunar Space Important to the Simulation of Space Vehicles. [Preprint] 2140-61, American Rocket Soc., Oct. 1961.

McCracken, Curtis W.: An Analysis of Rocket and Earth Satellite Measurements of Micrometeorite Influx. Final Report - Acoustic Detection of Meteoric Particles. AFCRC-TR-60-272, vol. II, Appendix B, Air Force Cambridge Res. Center, Apr. 14, 1960.

Olshaker, Arnold E.: An Experimental Investigation in Lead of the Whipple "Meteor Bumper." Jour. of Appl. Phys., vol. 31, no. 12, Dec. 1960, pp. 2118-2120.

Pereira, John F.: The Effect of Meteoroids on the Structural Design of Space Vehicles. Rep. No. RDSR-7, Republic Aviation Corp., June 1960.

Rinehart, J. S.: Meteor Distribution and Cratering. Proc. of Second Hyper-velocity Impact Symposium, vol. 1, W. C. Mannix, W. W. Atkins, and R. E. Clark, eds., Dec. 1957, pp. 45-53. (Sponsored by U.S. Naval Res. Lab. and Air Res. and Dev. Command.)

Rodriguez, David: Meteoroid Shielding for Space Vehicles. Aerospace Engineering, vol. 19, no. 12, Dec. 1960, pp. 20-23, 55-66.

Shaw, J. H.: Natural Environment of Interplanetary Space. Ohio State Univ. Res. Foundation, Jan. 1960. (Available from ASTIA as AD-250-230.)

Wallace, R. R., Jr., Vinson, J. R., and Kornhauser, M.: Effects of Hypervelocity Particles on Shielded Structures. [Preprint] 1683-61, American Rocket Soc., Apr. 1961.

Whipple, Fred L.: Dust and Meteorites. [Preprint] 2253-61, American Rocket Soc., Oct. 1961.

TABLE I.- RELATIVE ABUNDANCE OF ELEMENTS IN THE UNIVERSE

[From reference 12]

Element	Relative abundance
Hydrogen	1,000
Helium	79
Oxygen	0.5
Neon	0.2
Nitrogen	0.2
Carbon	0.06
Magnesium	0.04
Silicon	0.03
Iron	0.02
Sulphur	0.01
Argon, fluorine, sodium, calcium, nickel, and aluminum	~0.002 each

TABLE II - WHIPPLE'S 1957 ESTIMATE OF THE METEORITIC FLUX AND ESTIMATES OF THE PENETRATION POTENTIAL USING VARIOUS PENETRATION EQUATIONS[a]

Meteor visual magnitude	Mass, g (b)	Radius, microns	Assumed velocity, km/sec	Impacts m^2-sec	Number meteors striking earth per day	Assumed velocity, ft/sec	Impacts ft^2-day	Thickness of Al sheet required to prevent penetration, in.	
								Charters and Summers (c)	Bjork (c)
0	25 0	49,200	28	$5\ 27 \times 10^{-14}$	----------	9.19×10^{4}	$4\ 23 \times 10^{-10}$	10 9	5 719
1	9.95	36,200	28	$1\ 324 \times 10^{-13}$	----------	9 19	$1\ 063 \times 10^{-9}$	8 03	4 205
2	3 96	26,600	28	3.33×10^{-13}	----------	9 19	$2\ 67 \times 10^{-9}$	5 90	3 098
3	1.58	19,600	28	$8\ 34 \times 10^{-13}$	----------	9 19	6.69×10^{-9}	4 34	2 280
4	.628	14,400	28	$2\ 10 \times 10^{-12}$	----------	9 19	$1\ 69 \times 10^{-8}$	3 20	1 674
5	250	10,600	28	$5\ 27 \times 10^{-12}$	2×10^{8}	9.19	4.23×10^{-8}	2 35	1 230
6	$9\ 95 \times 10^{-2}$	7,800	28	$1\ 324 \times 10^{-11}$	5.84×10^{8}	9.19	$1\ 063 \times 10^{-7}$	1 73	908
7	$3\ 96 \times 10^{-2}$	5,740	28	$3\ 33 \times 10^{-11}$	1.47×10^{9}	9 19	$2\ 67 \times 10^{-7}$	1.27	663
8	$1\ 58 \times 10^{-2}$	4,220	27	8.34×10^{-11}	3.69×10^{9}	8.86	$6\ 69 \times 10^{-7}$	.913	485
9	$6\ 28 \times 10^{-3}$	3,110	26	$2\ 10 \times 10^{-10}$	$9\ 26 \times 10^{9}$	8.53	$1\ 69 \times 10^{-6}$	658	352
10	$2\ 50 \times 10^{-3}$	2,290	25	5.27×10^{-10}	$2\ 33 \times 10^{10}$	8.20	$4\ 23 \times 10^{-6}$	470	256
11	$9\ 95 \times 10^{-4}$	1,680	24	$1,324 \times 10^{-9}$	$5\ 84 \times 10^{10}$	7.87	1.063×10^{-5}	.336	185
12	$3\ 96 \times 10^{-4}$	1,240	23	$3\ 33 \times 10^{-9}$	1.47×10^{11}	7 55	$2\ 67 \times 10^{-5}$	241	135
13	$1\ 58 \times 10^{-4}$	910	22	$8\ 34 \times 10^{-9}$	3.69×10^{11}	7 22	6.69×10^{-5}	172	0972
14	$6\ 28 \times 10^{-5}$	669	21	2.10×10^{-8}	9.26×10^{11}	6 89	$1\ 69 \times 10^{-4}$	123	0708
15	2.50×10^{-5}	492	20	$5\ 27 \times 10^{-8}$	$2\ 33 \times 10^{12}$	6 56	4.23×10^{-4}	0871	0493
16	9.95×10^{-6}	362	19	1.324×10^{-7}	$5\ 84 \times 10^{12}$	6 23	$1\ 063 \times 10^{-3}$	0618	0370
17	$3\ 96 \times 10^{-6}$	266	18	$3\ 33 \times 10^{-7}$	1.47×10^{13}	5 91	$2\ 67 \times 10^{-3}$	0441	0267
18	$1\ 58 \times 10^{-6}$	196	17	$8\ 34 \times 10^{-7}$	$3\ 69 \times 10^{13}$	5 58	6.69×10^{-3}	0311	0193
19	$6\ 28 \times 10^{-7}$	144	16	$2\ 10 \times 10^{-6}$	$9\ 26 \times 10^{13}$	5 25	$1\ 69 \times 10^{-2}$	0220	0139
20	$2\ 50 \times 10^{-7}$	106	15	$5\ 27 \times 10^{-6}$	$2\ 33 \times 10^{14}$	4 92	$4\ 23 \times 10^{-2}$	0155	00998
21	9.95×10^{-8}	78 0	15	$1\ 324 \times 10^{-5}$	$5\ 84 \times 10^{14}$	4.92	1.063×10^{-1}	0114	00734
22	3.96×10^{-8}	57.4	15	3.33×10^{-5}	$1\ 47 \times 10^{15}$	4 92	2.67×10^{-1}	.00840	00542
23	1.58×10^{-8}	[d]39 8	15	$8\ 34 \times 10^{-5}$	3.69×10^{15}	4 92	6.69×10^{-1}	.00617	00399
24	6.28×10^{-9}	[d]25.1	15	2.10×10^{-4}	9.26×10^{15}	4.92	1.69	00456	00293
25	2.50×10^{-9}	[d]15 8	15	$5\ 27 \times 10^{-4}$	$2\ 33 \times 10^{16}$	4 92	4 23	00334	00216
26	9.95×10^{-10}	[d]10 0	15	1.324×10^{-3}	$5\ 84 \times 10^{16}$	4 92	10 63	00246	.00158
27	3.96×10^{-10}	[d]6 30	15	$3\ 33 \times 10^{-3}$	1.47×10^{17}	4 92	26 7	.00182	00117
28	1.58×10^{-10}	[d]3.98	15	8.34×10^{-3}	3.69×10^{17}	4 92	66 9	.00133	000857
29	$6\ 28 \times 10^{-11}$	[d]2 51	15	2.10×10^{-2}	9.26×10^{17}	4 92	169	.000977	.000631
30	$2\ 50 \times 10^{-11}$	[d]1 58	15	5.27×10^{-2}	$2\ 33 \times 10^{18}$	4.92	423	.000720	000464
31	$9\ 95 \times 10^{-12}$	[d]1 00	15	$1\ 324 \times 10^{-1}$	5.84×10^{18}	4.92	1,063	000527	.000341

[a]Parts of this table are from reference 2

[b]Whipple's 1961 estimate differs from this table in that the masses of particles between +0 and +4 visual magnitude are reduced by a factor of 10 A constant reduction of a factor of 10 is used for all particles in this report when referring to Whipple's 1961 estimate

[c]A meteroid density of 2 7 g/cm^3 was assumed for the values shown in this column. This column applies only to Whipple's 1957 estimate of the mass distribution (see footnote b)

[d]Particles with these radii have densities greater than 0 05 g/cm^3 to preclude elimination from the solar system due to solar pressure.

TABLE III - METEOROID ENVIRONMENT STUDIES

NASA or USAF No	Contractor	Title or Description	Period
--------	NASA M I T - Lincoln Labs	Trailblazer - High-speed injection of known particles into the atmosphere to simulate meteors	----------
--------	NASA	S-55 - Hollow pressurized beryllium copper cylinders to record meteoroid punctures; stainless-steel sheet backed with grid	Launched Aug 25, 1961, reentry Aug 27, 1961
--------	NASA	Explorer I - Microphone micrometeoroid detectors	Launched Jan 31, 1958, no longer transmitting
--------	NASA	Explorer VIII - Microphone micrometeoroid detectors	Launched Mar 26, 1958, no longer transmitting
--------	NASA	Vanguard III - Microphone micrometeoroid detectors.	Launched Sept 18, 1959, no longer transmitting
NsG-58	University of Maryland	Theoretical studies on interplanetary gas and dust	Feb 1960 to Jan 1963
NsG-71	Smithsonian Institution	Tektite collection and study	Apr 1960 to Mar 1962
NsG-82	Yale University	Steady-state interaction between radiation and matter in stellar atmospheres	June 1960 to June 1961
NsG-113	Rensselaer Polytechnic Institute	Models of interstellar dust clouds and extinction and polarization in the ultraviolet	Nov. 1960 to Nov 1962
NsG-121	Stanford University	Radar studies of 15th magnitude meteors during satellite count periods	Nov 1960 to May 1961
NsG-128	University of Chicago	Low-level gamma counting equipment for research on cosmic-ray induced radio-activity in meteorites	Jan 1961 to Jan 1962
NaSr-7	Oklahoma State University	Study of mechanisms of impact penetration and light emission for micrometeorites on an aluminum-coated photomultiplier	Oct 1960 to Sept. 1961
--------	Pennsylvania State University	Investigation of helium contents of meteorites	June 1959 to May 1960
NsG-84	Temple University	Production of hypervelocity particles of small size and increase in the sensitivity of micrometeorite detection techniques (statistical methods of data interpretation)	Sept 1960 to Sept. 1962
NASw-158	Nebraska Historical Society	Examination of newspapers covering the period of 1915 meteor shower	Apr 1960 to May 1960
NAS 5-664	A D Little, Inc.	Measurement of meteoroid damage to propellant tanks	----------
--------	Bucknell University	Statistical analysis procedures for analyzing data (Lewis Research Center)	----------
NASr-75	General Dynamics Corp.	Neutron and photoneutron analyses of meteorites to determine rare-earth homogeneities.	2 years
NASr-49(03)	Stanford Research Institute	Determine the general shape and condition of Echo I satellite by means of direct high-resolution photography.	Nov. 1, 1961 to Feb 28, 1962

TABLE III - METEOROID ENVIRONMENT STUDIES - Concluded

NASA or USAF No	Contractor	Title or Description	Period
NsG-187-62	Lawrence College	Literature search for accounts for a particular group of fireballs - the Cyrillids.	4 months
USAF (770A) Proj 7667	Geophysics Res Div. Cambridge Res Labs.	"METEOR PHYSICS"	---
Task 76030	University of British Columbia Device Dev. Corp. Harvard College Perkin-Elmer Corp.	Meteor train photography· study of meteoric physics by visual and optical techniques.	---
Task 76045	University of Manchester, Jodrell Bank	Radio meteor studies study meteors and ionization trails by the scattering of pulse and CW electromagnetic radiation in frequency range up to 200 mc/sec.	---
Task 76046	Smithsonian Institution Astro. Laboratory Research Services, Inc Dudley Observatory Temple University Geo-Service, Inc Oklahoma State University Northeastern University Max Plank Institute Wentworth Institute	Rocket and satellite meteor studies: measure influx rate, velocity, radiant and potential damage and spatial density as a function of distance from the earth	---
Task 76671	Stanford Research Institute General Mills, Inc A D Little, Inc	High-speed impact phenomena: calibration of meteoric detectors (shaped charges and guns).	---
Proposals			
406	Battelle Memorial Institute	Analysis of deformation structures in iron meteorites.	12 months
909	Department of Interior	U.S. geological survey investigation of tektites and meteorites	16 months
1156	University of Florida	Study on the origin of meteorites	36 months
1263	Smithsonian Institution	Collection and analysis of extra-terrestrial dust	12 months
1237	University of Arkansas	Trace elements in meteorites and the age of the solar system	12 months
488	M I. T.	Radar for outer-space research	12 months
1490	University of Minnesota	Studies of alkali and alkaline earth elements in stone meteorites	12 months
1309 1556	Smithsonian Institution	Photo observation of meteorites in flight and their subsequent recovery.	36 months
1771	Boston University	Research into the problems of tektites and space environment of the earth (continuation of NsG-21).	12 months
1809	Advanced Kinetics, Inc	Behavior of macroscopic particles under the influence of electromagnetic fields.	12 months
1119	Dudley Observatory	Study of micrometeorite sizes.	4 months
1557	ARDC Cambridge	Cosmic dust collector.	---
---	Lincoln Laboratories M I T	Calibration of radar system against photographic visual magnitude by simultaneous observation of a natural meteor	---

TABLE IV - POSTULATED EMPIRICAL EQUATIONS[1]

Penetration law	Target	Projectile	Shape	Size	Velocity	Reference
$\bar{P} = \left(\frac{3K_1K_2}{2\pi}\right) V_p^{1/3} \left(\frac{\rho_p}{\rho_t}\right)^{1/3} \left(\frac{V}{c_t}\right) \frac{1}{\left(3 - K_2 \frac{V}{c_t}\right)}$	Aluminum Wax (10° C) Brass Lead Magnesium Steel Zinc	} Aluminum Brass Lead Magnesium Steel Zinc	Spheres	1/8 in	$\frac{V}{c_t} \leq 1$	77
$\frac{\bar{P}}{d} = 2\,5 \left(\frac{V}{c_t}\right)^{1.4}$	Aluminum Brass Lead Magnesium Magnesium-lithium Lead	Aluminum Brass Lead Magnesium Magnesium-lithium Lead	Spheres Cylinders	1/8 in	$0\,1 \leq \frac{V}{c_t} \leq 1\,0$	57
$P = K \frac{m_p^{1/3} V^{1/3}}{\rho_t^{1/6} H^{1/4}}$	Aluminum Brass Bronze Copper Mallory Steel Titanium	----------	Jet	----------	10,540 fps	78
	Lead	Steel	Disc	----------	1,300 fps to 15,400 fps	55
$\bar{P} = \frac{V_p \left(1 - e^{-K_4 E}\right)}{K_1 K_3 \left(2 m_p E\right)^{1/2} + K_2}$	Lead	Lead	Spheres	$\frac{1}{8}$ in , $\frac{3}{16}$ in , $\frac{3}{8}$ in	<5,900 fps	79
$\bar{P} = K m_p^{1/3} \frac{(V - V_o)}{c_t}$ $\frac{V_o}{c_t} < \frac{V}{c_t} < 2$	Wax (23° C)	Wax (4° C)	Spheres Cylinders	0 177 in } d = 0 22 in L = 0 33 in } d = 0 222 in L = 0 388 in	$0\,3 < \frac{V}{c_t} < 2\,2$	80
$\frac{\bar{P}}{d} = K \left(\frac{V}{\bar{c}_p}\right)^{\bar{c}_t / \bar{c}_p}$	Aluminum Copper Lead Steel Tin	} Aluminum Copper Mallory 1000 Steel	Fragments	----------	1,000 fps to 6,000 fps	56

[1]Information in this table was obtained from reference 10 Symbols and reference numbers have been changed to conform to notation in the present paper

TABLE IV - POSTULATED EMPIRICAL EQUATIONS[1] - Concluded

Penetration law	Target	Projectile	Shape	Size	Velocity	Reference
$\frac{P}{d} = \frac{7\ 2\bar{c}_p\rho_p}{\bar{c}_t\rho_t + \bar{c}_p\rho_p}\left(\frac{V}{\bar{c}_p}\right) - \frac{136\ 8\sigma_y\rho_p^{1/2}}{\bar{c}_t^{\,2}\rho_t^{3/2}}$	Aluminum 1100 Aluminum 2024-0 Copper Lead Steel	Mercury	Spheres	----------	<6,500 fps	81
	Aluminum 2024-0 Copper Lead	Water				
1 5d ≦ target thickness ≦ 5d	Aluminum Copper Iron Lead Zinc	Aluminum Copper Iron Lead Zinc				
$\frac{P}{d} = 2\ 28\left(\frac{\rho_p}{\rho_t}\right)^{2/3}\left(\frac{V}{c_t}\right)^{2/3}$	Copper Lead	Aluminum Copper Lead Magnesium-lithium Steel Tungsten	Spheres	0.125 in , 0 178 in 0 125 in , 0 119 in 0 125 in , 0 109 in 0 125 in , 0 218 in 0 125 in , 0 125 in , 0 096 in	≦11,000 fps	82
	Aluminum Magnesium Nickel Polyethylene Stainless steel	Stainless steel	Microparticles	100μ and 150μ	2,300 fps to 13,200 fps	83
$\frac{P}{d} = 1\ 9\left(\frac{\rho_p}{\rho_t}\right)\left(\frac{V}{c_t}\right)$	Aluminum Steel Steel	Aluminum Magnesium	Spheres	0 2 in , 0 4 in	≦17,700 fps	84
$\frac{P}{d} = 2\left(\frac{V}{\bar{c}_t}\right)^{3/4}$	Steel	Steel	Spheres	0 2 in		
$\frac{P}{d} = 2\ 8\left(\frac{\rho_p}{\rho_t}\right)^{0\ 8}\left(\frac{V}{\bar{c}_t}\right)^{0\ 7}$	Copper Lead	Aluminum	Spheres	0 2 in , 0 4 in		
$P = \frac{622\left(\rho_p VL - 6.89 \times 10^{-3}b\right)}{\left(\rho_p\right)^{0.278}\left(E + 1.93 \times 10^{10}\right)^{0\ 78}}$	Aluminum Copper Lead Steel	Aluminum Copper Lead Steel	Spheres Cylinder (L/d = 1)	0.0620 in 0 22 in. 0 50 in. 0 22 in 0 50 in	≦13,000 fps	63
$P = \frac{K}{2} m_p^{1/3} v^{2/3}$	Cadmium Copper Lead Zinc	----------	----------	----------	----------	85
$P = \left(\frac{3}{4\pi K}\right)^{1/3} \frac{m_p^{1/3} v^{2/3}}{H^{1/3}}$	Aluminum Copper Steel	----------	----------	----------	----------	85

[1]Information in this table was obtained from reference 10 Symbols and reference numbers have been changed to conform to notation in the present paper

TABLE V - HYPERVELOCITY IMPACT STUDIES

NASA of USAF No.	Contractor	Title or Description	Period
NASw-14	Pennsylvania State University	Theoretical investigation of stress penetration waves and impact damage in plates	Dec 1958 to Dec 1959
NsG-66	Pennsylvania State University	Continuation of NASw-14	Jan 1960 to Dec 1961
----------	NASA - Ames	Impact studies - bumper and heat-shield materials	----------
----------	NASA - Langley	Impact studies - bumper and porous projectiles, theoretical studies, microparticle electrostatic accelerator, exploding-metal techniques	----------
----------	NASA - Lewis	Effect of hypervelocity impact on the catastrophic failure of propellant tanks, impact into thin-walled liquid containers	----------
NASr-7	Oklahoma State University	Analytical and experimental study of the mechanisms of impact, penetration and light emission for micrometeorites on an aluminum-coated photomultiplier	Oct 1, 1960 to Sept 30, 1962
USAF (740A)Proj 5841	WADD and AFGC	Hypervelocity Impact Studies	Nov 1958 to present
Task 584101	Aerojet-General Corp and Utah Research & Development Company	Hypervelocity Impact Data Acquisition to collect hypervelocity-impact data through in-house effort, from other DOD agencies and by contract effort.	Nov 1958 to present
Task 584102	----------	Analysis of hypervelocity impact data from all sources	Nov 1958 to present
USAF (740A)Proj 2835	ASD Detachment 4, Eglin Air Force Base	Advanced nonnuclear warheads	----------
Task 283502	In-house	Lethality studies to determine relative behavior of various types of fragments when impacted against representative targets at hypervelocities Factors such as depth of penetration, size of perforation, carry-through back spall, fragment breakup, chemical reaction will be determined	Indefinite
USAF (740A)Proj 5218	----------	Hypervelocity interceptor guidance and control techniques (ASD Project)	----------
Task 521805	Aerojet-General, Corp and Wright Patterson in-house	Hypervelocity fragment damage collect, analyze, assess impact data on non-functioning missile components - determine minimum mass lethality in relation to ICBM's - prepare "Handbook" data	June 1960 to present
Task 521806	Aerojet-General Corp. and Wright Patterson in-house	Nonnuclear kill mechanisms	June 1960 to present
USAF (806A)Proj 9860	ASD Detachment 4, Eglin Air Force Base	Research in viscous mechanics under extreme conditions	----------
Task 986002	Space Technology Laboratories and Wright Patterson in-house	Change in very high velocity impact phenomena with hyperstrength particles to observe the effects of hypervelocity impact of particles having strengths of the same order as the impact pressures encountered	July 1960 to present

TABLE V - HYPERVELOCITY IMPACT STUDIES - Concluded

NASA or USAF No	Contractor	Title or Description	Period
Task 986003	General Electric Co (Phila) and Hayes Corp. (Birmingham)	Theory of High-Speed Impact to study the behavior of materials under certain conditions of high rate of strain. (PGWR of APGC)	July 1960 to present
USAF (802A)Proj 7021	----------	Solid-state research and properties of matter (ARL)	----------
Task 73650	National Bureau of Standards	Particle-solid impact phenomena understanding the phenomena occurring during the impact of solid particles against solids In particular, liquid-to-liquid collision theory validity will be investigated	0 3 man year
USAF (801A)Proj 9751	----------	Research in energy release processes (OSR)	----------
Task 37511	Smithsonian Observatory, University of Utah	Research in physics (Energetics) meteorite collection measurements and cratering dynamics	----------
USAF (750A)Proj 8871	Arnold Engineering Development Center, APGC (Eglin Air Force Base)	Hypervelocity projector techniques (management)	5 man years/year
Task 88712	Utah Research and Development Company and Colorado Seminary, University of Denver	Light-gas projectors. to provide research and development for projector techniques for impact studies	----------
1299	North American Aviation	Study of physics of meteoroid impact	12 months
1300	North American Aviation	Evaluation of satellite surface materials and structures for protection against meteoroid impact.	12 months
674	Lockheed Aircraft Corp.	Study of ultra light-weight structures for space application.	12 months
NSG-84-60	Temple University	Application of exploding wire and electrostatic acceleration techniques to dust particle accelerator to reach 80 to 100 km/sec for 10 to 100μ particles.	----------
----------	Naval Research Laboratories	Hypervelocity impact - includes development work on light-gas gun with electrical discharge augmentation	----------
----------	Lincoln Labs , M I T	Hypervelocity data acquisition and analysis (semi-infinite targets).	----------
----------	AVCO Corp	Hypervelocity impact includes electric discharge augmented light-gas gun	----------
----------	General Electric (in-house)	Bumper shields.	----------
----------	Ballistics Research Laboratories	Accelerated beryllium slugs; meteor bumpers; very thin material puncture, development of gun to fire artificial meteors back into atmosphere	----------
----------	North American Aviation, Inc.	Development of exploding metal gun to exceed 40,000 fps, already have surpassed 30,000 fps.	----------
----------	Technical Operations, Inc	Exploding metal 53,000 fps. Electric storage capacity being increased	----------

TABLE VI.- PARTIAL LIST OF HIGH-VELOCITY IMPACT FACILITIES

LABORATORY	TYPE OF FACILITY
Aerojet-General Corp. Azusa, California	Shaped charge Light-gas gun
U.S. Air Force Tullahoma, Tenn.	Light-gas guns
U.S. Air Force Cambridge Research Laboratory Bedford, Mass.	Explosive gun
Air Research and Development Establishment Fort Halstead, England	Shaped charge Light-gas gun
Armour Research Foundation Chicago, Ill.	Light-gas gun
AVCO Corp. Wilmington, Mass.	Light-gas gun Electric gas gun Powder guns
Ballistic Research Laboratories Aberdeen, Me.	Shaped charge Light-gas gun
The Boeing Co. Seattle, Washington	Just setting up range
Canadian Armament Research and Development Establishment	Powder gun Light-gas gun
Carnegie Institute of Technology Pittsburgh, Pa.	Shaped charge
Colorado School of Mines	Powder gun
General Dynamics/Convair San Diego, Calif.	Light-gas gun Electric gun Shaped charge
Cook Electric Company Morton Grove, Ill.	Explosives

TABLE VI.- PARTIAL LIST OF HIGH-VELOCITY IMPACT FACILITIES - Continued

LABORATORY	TYPE OF FACILITY
Denver Research Inst.	Light-gas gun Shaped charge
Frankford Arsenal Philadelphia, Pa.	Multistage high explosive gun
General Electric Co. Philadelphia, Pa.	Shaped charge Two stage high explosive gun
G. M. Defense Research Div. Santa Barbara Lab. Santa Barbara, Calif.	Light-gas gun Shaped charge
Grumman Aircraft Corp. Bethpage, N. Y.	Proton-charged microparticles
Lincoln Laboratory, M. I. T.	Powder gun Light-gas gun
M. I. T. Dept. Aero and Astronautics	Powder gun
NASA - Ames Research Center	Powder gun Light-gas gun
NASA - Langley Research Center	Powder gun Light-gas gun Explosives
NASA - Lewis Research Center	Light-gas gun under construction Powder guns
Naval Ordnance Test Station Inyokern, Calif.	Powder gun Light-gas gun
Naval Research Lab. Washington, D.C.	Powder gun Light-gas gun
Naval Ordnance Lab. White Oak, Md.	Light-gas guns Powder guns Explosives
North American Aviation, Inc. Downey, Calif.	Exploding metal

TABLE VI.- PARTIAL LIST OF HIGH-VELOCITY IMPACT FACILITIES - Concluded

LABORATORY	TYPE OF FACILITY
Picatinney Arsenal Dover, N. J.	Shaped charge Light-gas guns Powder guns
Ramo-Wooldridge Corp. Cunoga Park, Calif.	Electrostatic accelerator
Rheem Mfg. Corp. Downey, Calif.	Powder gun
Rhodes and Bloxsom, Inc.	Light-gas gun
Stanford Research Institute Poulter Laboratories Menlo Park, Calif.	Shaped charge
Technical Operations, Inc. Burlington, Mass.	Exploding wires and foils
University of Utah	Shaped charge Powder gun Light-gas gun Electromagnetic gun
Utah Research and Development, Inc.	Light-gas gun
Watertown Arsenal, Watertown, Mass.	Powder gun Light-gas gun

TABLE VII.- PARTIAL LIST OF PROPOSED METEOROID INVESTIGATIONS BY SPACE VEHICLES

Agency	Vehicle	Characteristics	Sensitivity range	Launch date
NASA - Goddard	Rockets	To study high-density, small-particle streams.	High sensitivity	Suitable for periodic events
NASA - Goddard	Rockets	60 km to 100 km to search for high concentrations of low-velocity small particles.	High sensitivity	Sporadic
NASA - Langley		Purpose to measure penetration flux in structural materials	Thin metal gages but near those for structural materials	1962
NASA		Penetration experiment. Details not formulated.	----------	
NASA - Goddard	Recoverable satellites on probes	Collection devices.	----------	1962 (?)
NASA - Goddard	Scout 12	Small-particle experiment.	----------	1962 (?)
NASA - Goddard	Lunar Orbiter	Probably similar to Explorer VIII	10^{-12} g to 10^{-7} g	1964 or 1965
NASA - Goddard	Venus probe	Near miss of Venus.	Probably high sensitivity	1962
NASA - Goddard	Mars probe	Measure spatial density, mass distribution, and variations.	Probably high sensitivity	1964
NASA - Goddard	Comet probe	Vehicle will be sent through comet head	Unknown	1964
NASA - Langley	Paraglider	Evaluation of Mylar meteoroid sensor. Capture of meteoroid dust during very high altitude glide Measurement of flux rate.	----------	1962 (?)
U.S. Air Force Cambridge Research Laboratory	Rockets	Altitude 40 miles and beyond.	Probably high sensitivity	1962
U.S. Air Force Cambridge Research Laboratory	Deep space	60 to 40,000 miles.	Probably high sensitivity	1962
U.S. Air Force Cambridge Research Laboratory	Orbital	Wires and imbedded mesh	Probably high sensitivity	1962

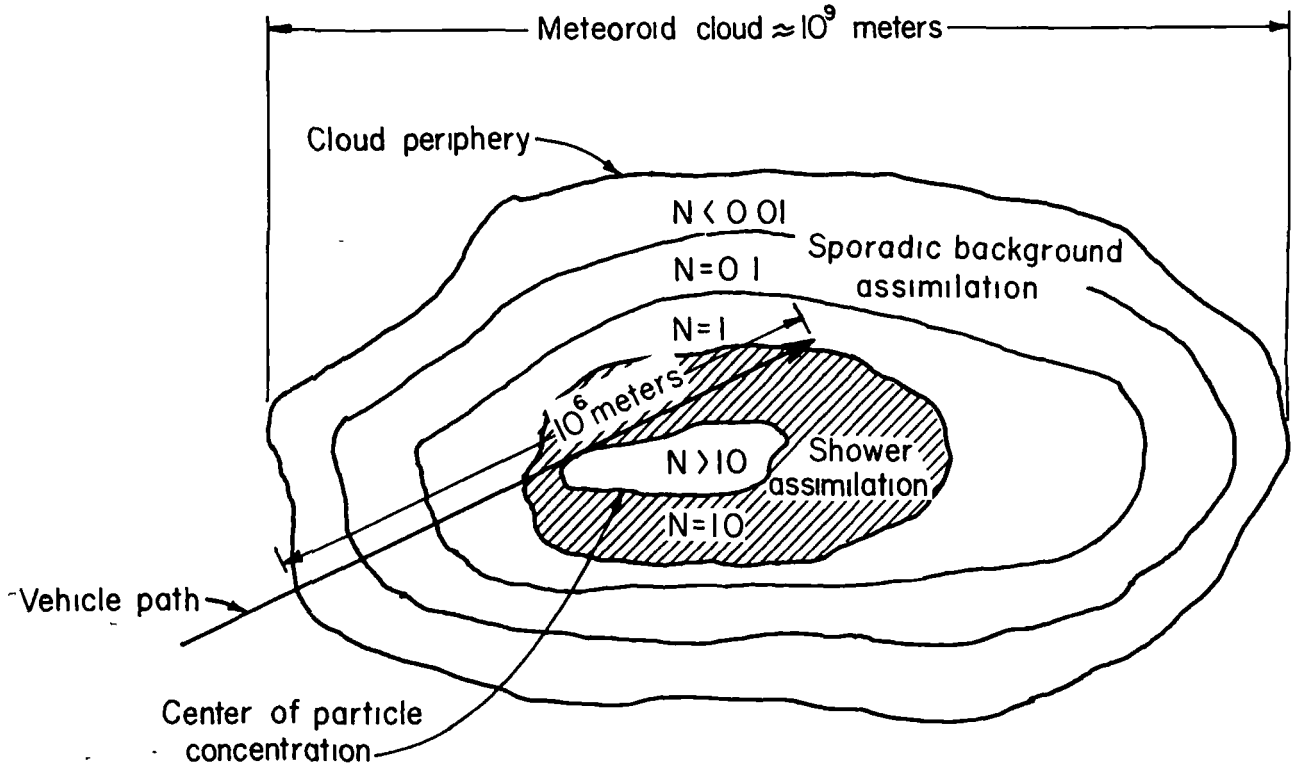

Figure 1.- Idealized meteoroid-cloud environment model. The relative number of meteoroid counts during a fixed time period is denoted by N. From reference 15.

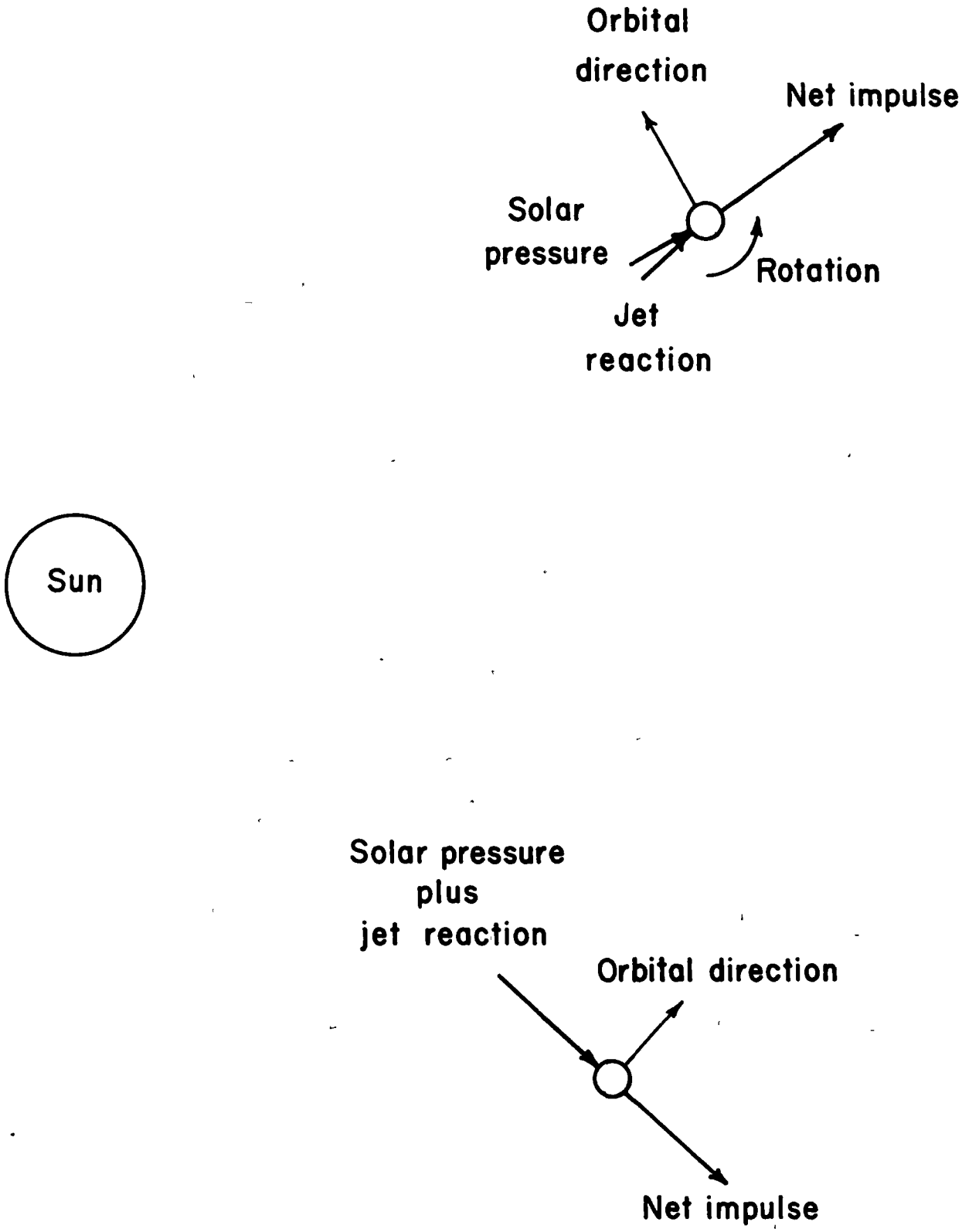

Figure 2.- The jet effect on cometary particle scattering.

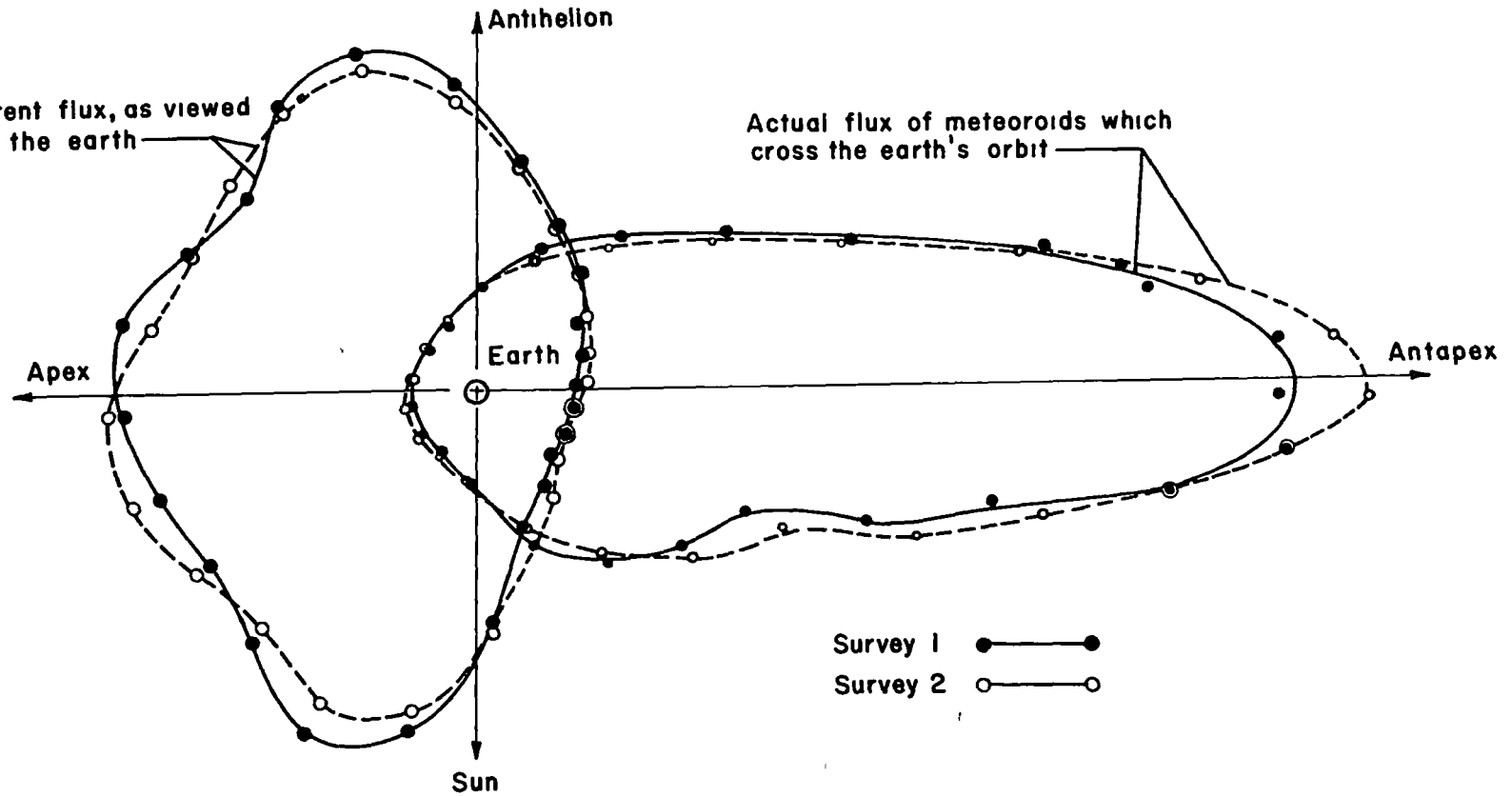

Figure 3.- Polar diagram drawn in the plane of the Earth's orbit which shows the apparent number of meteor radiants detected per unit angle, per second. From reference 86.

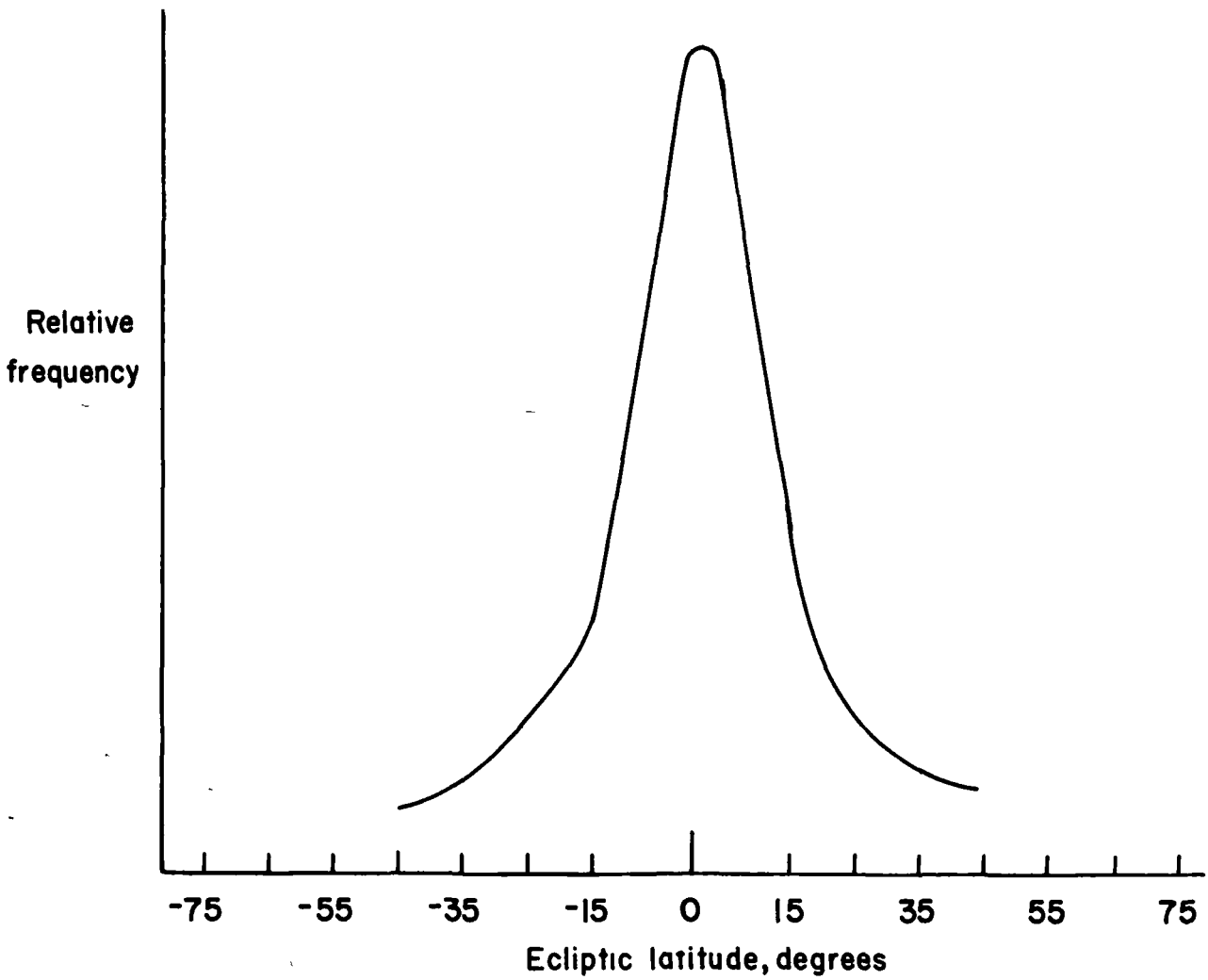

Figure 4.- Distribution of the meteor flux about the plane of the ecliptic at the Earth's distance from the Sun.

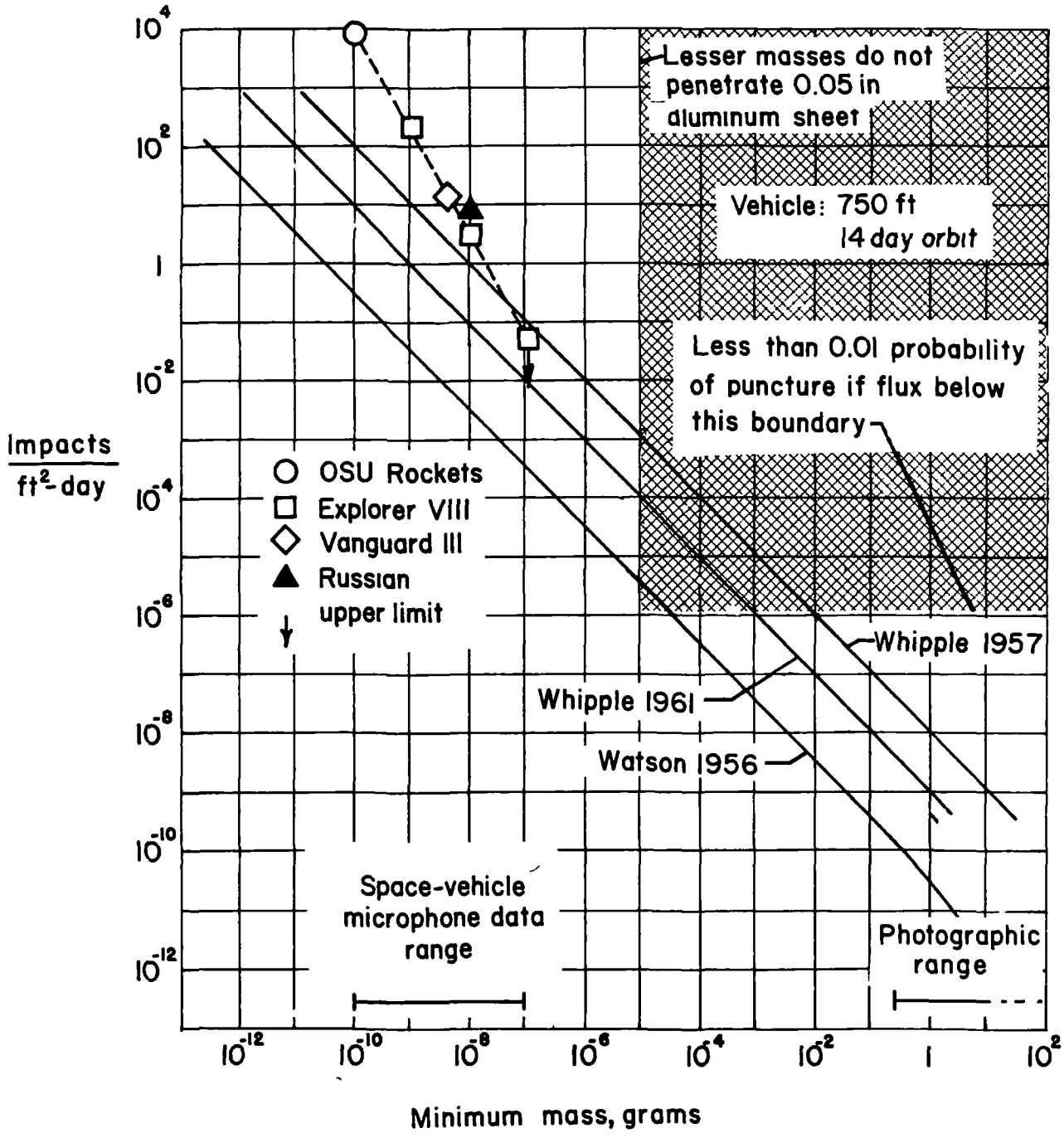

Figure 5.- Estimates of the meteoroid flux in the vicinity of the Earth.

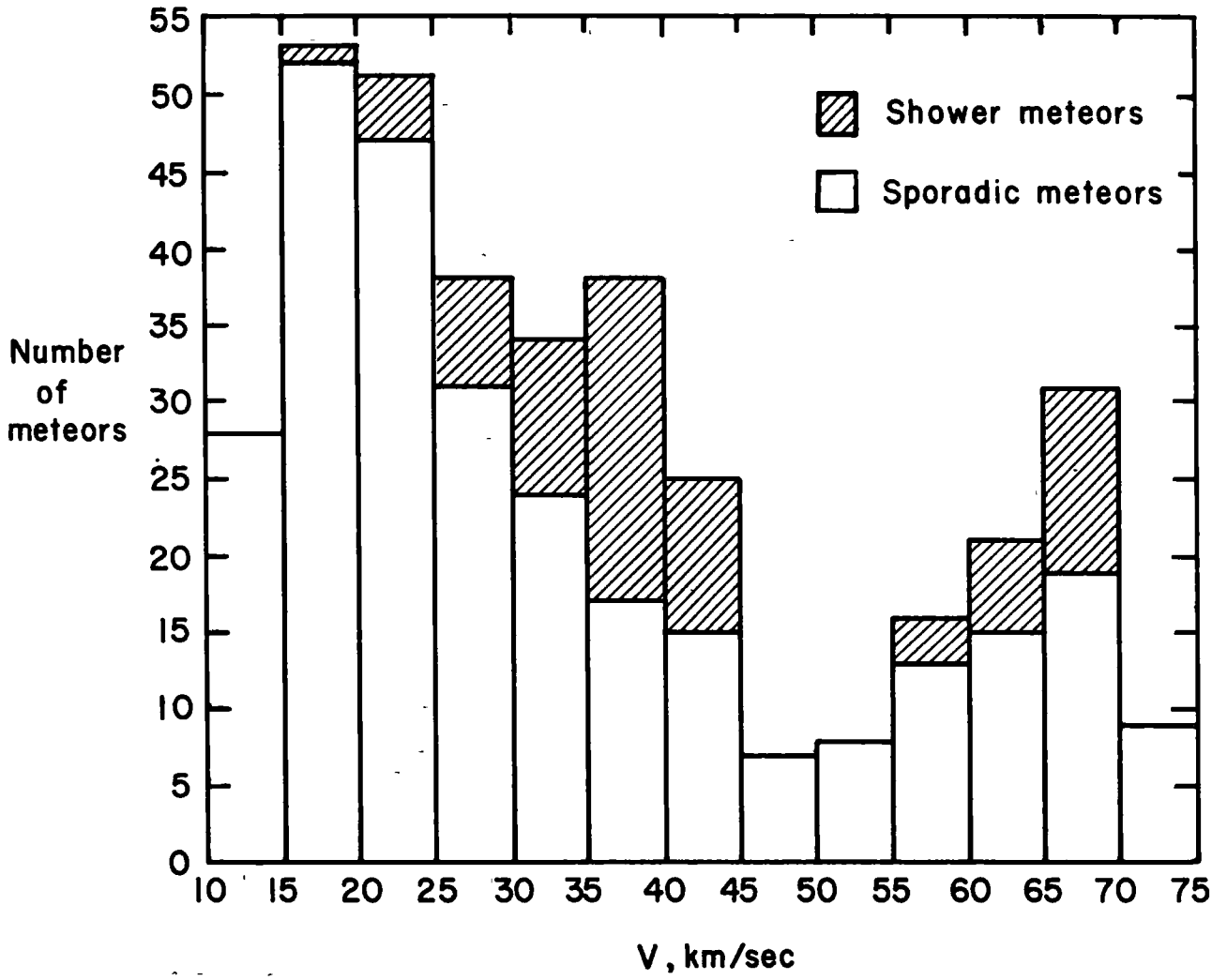

Figure 6.- Distribution of corrected velocities for 285 sporadic and 74 shower meteors. From reference 21.

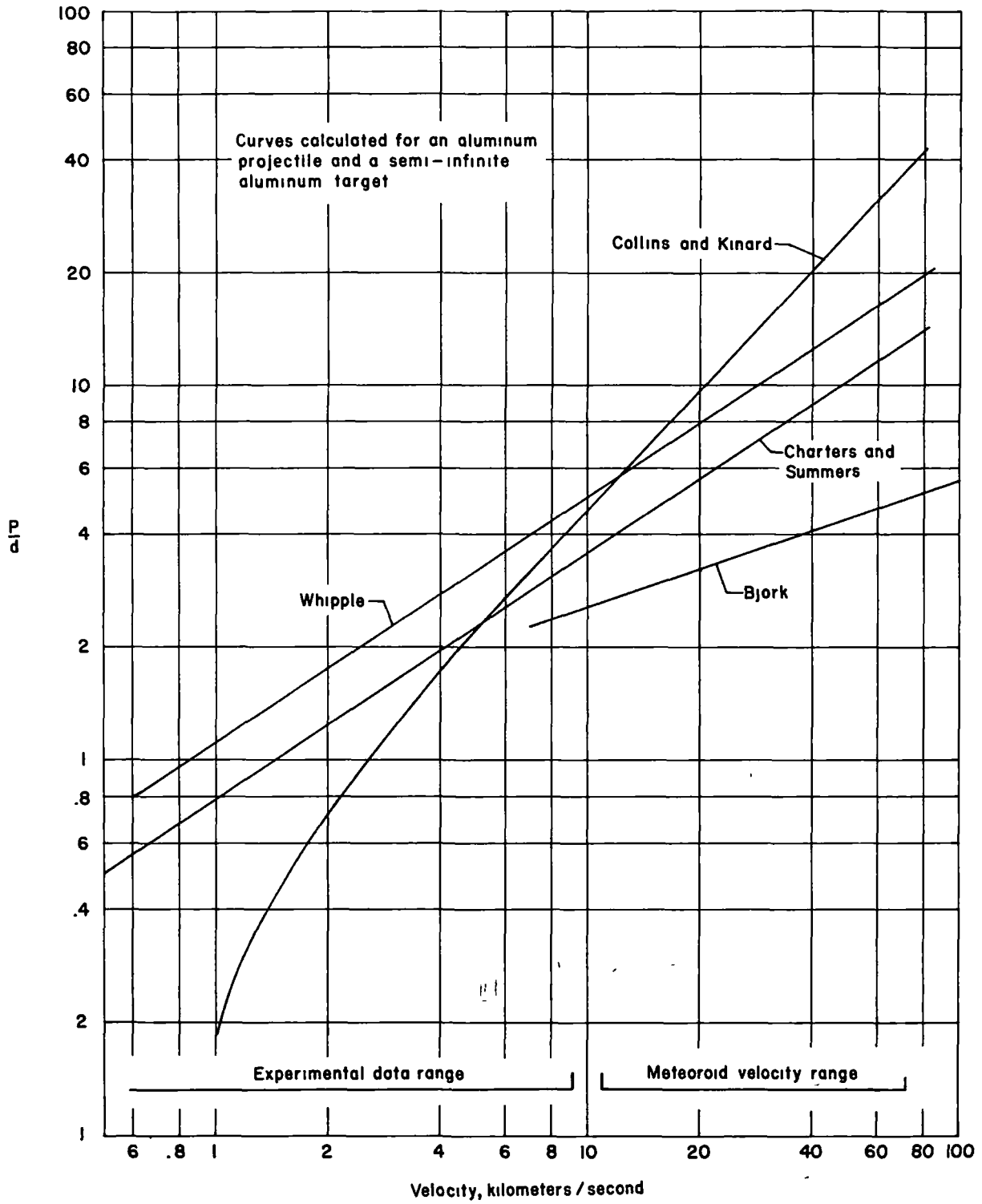

Figure 7.- The ratio of penetration depth to projectile diameter as a function of projectile velocity as predicted by various penetration formulas. Note that the empirical equations are extrapolated.

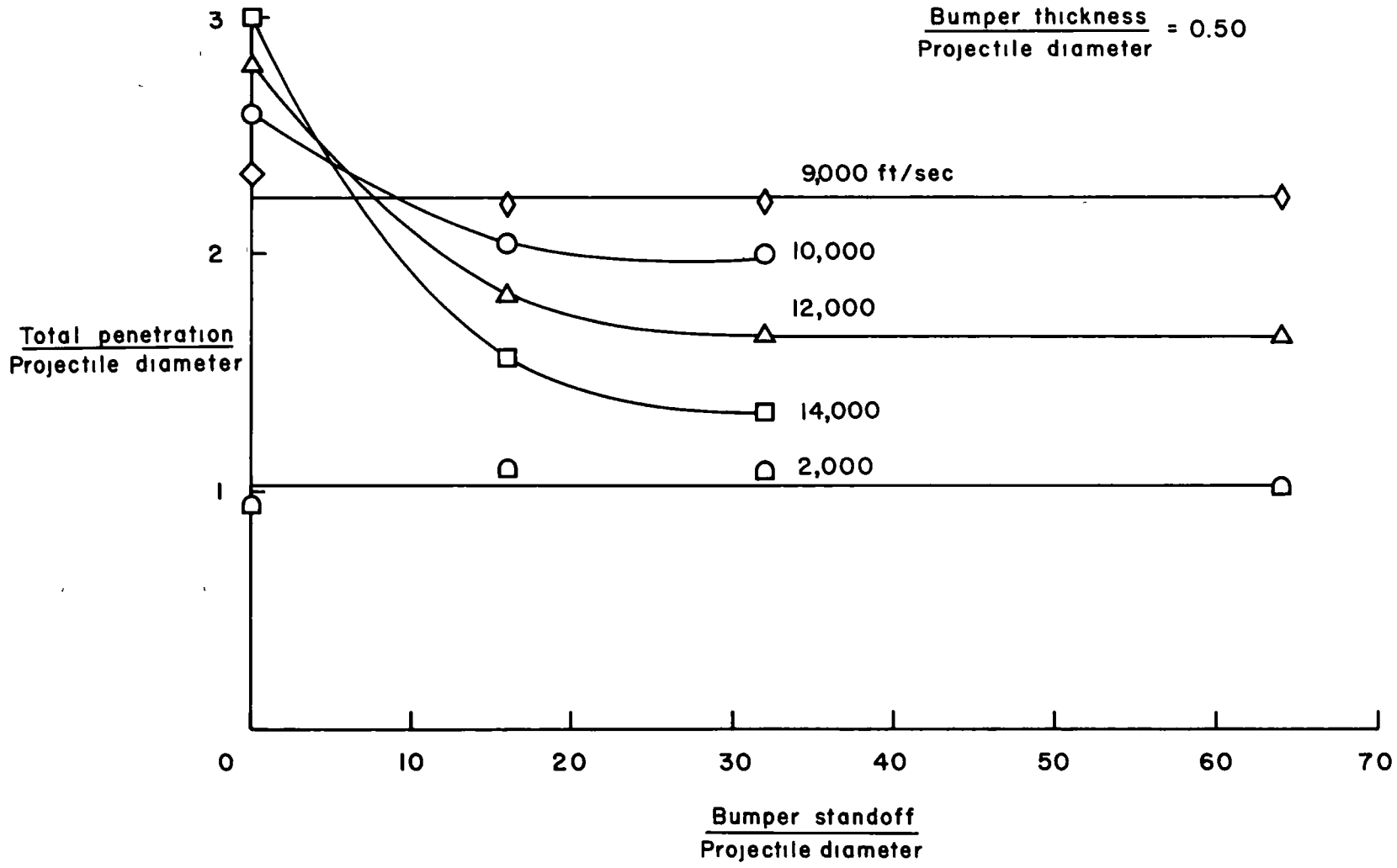

Figure 8.- Total penetration (bumper plus crater depth in quasi-infinite target) as a function of bumper standoff distance.

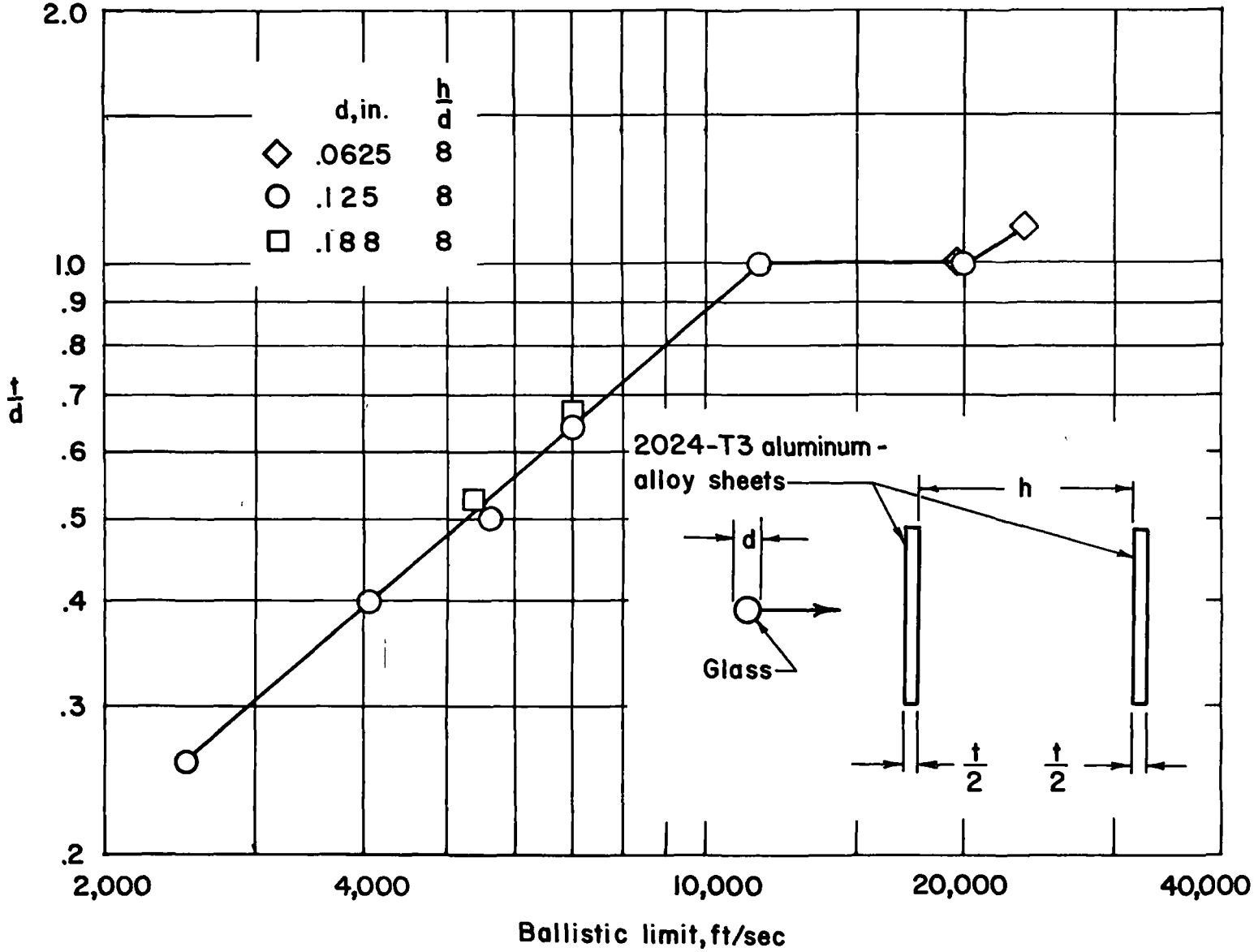

Figure 9.- Effect of thickness on the ballistic limit. The ballistic limit is the minimum velocity required to penetrate or rupture the rear sheet. From reference 72.

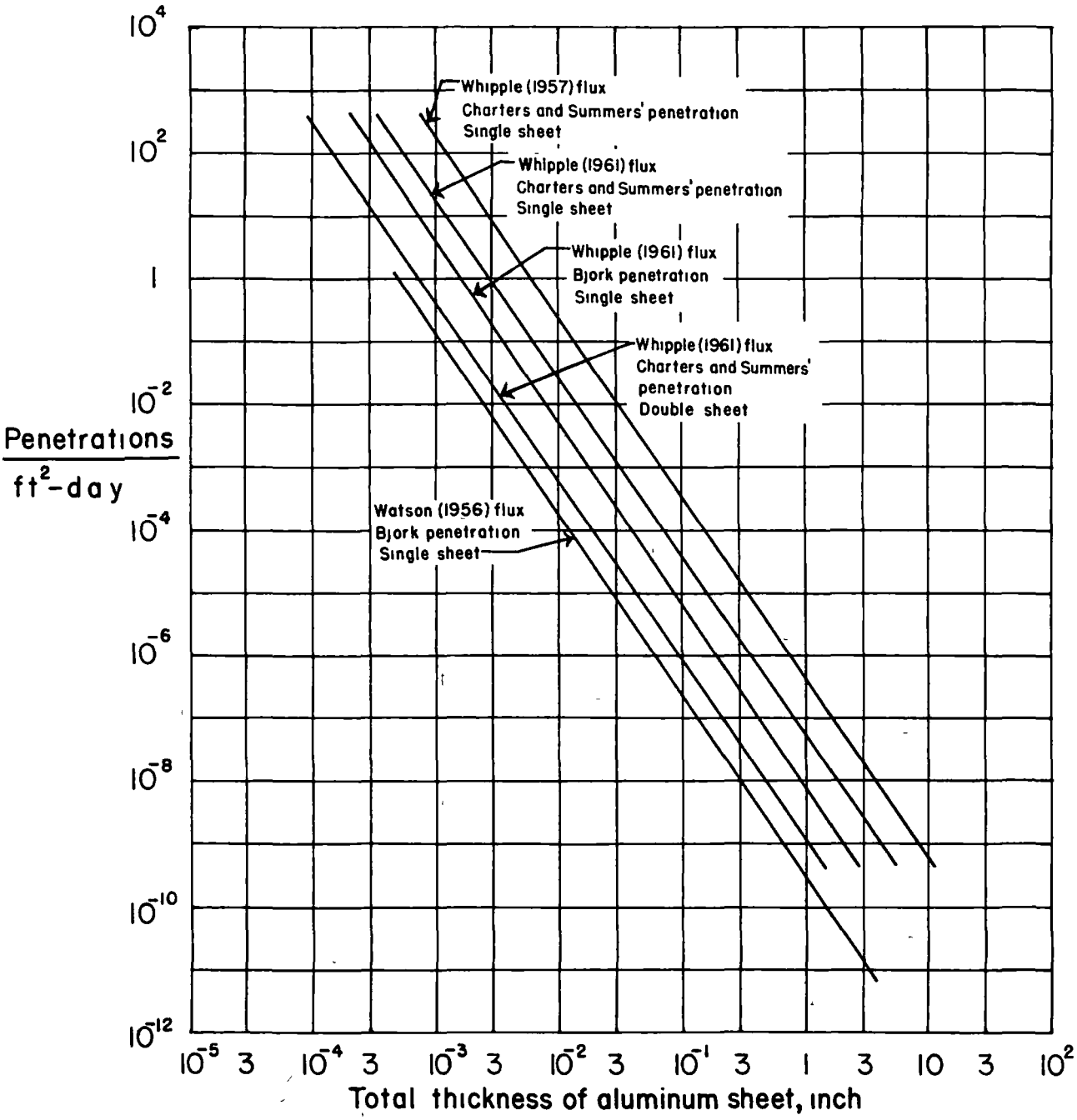

Figure 10.- Most probable rate of puncture as a function of total aluminum skin thickness as determined by various methods. For the purpose of comparison a meteoroid density of 2.7 g/cm^3 was assumed in all cases.

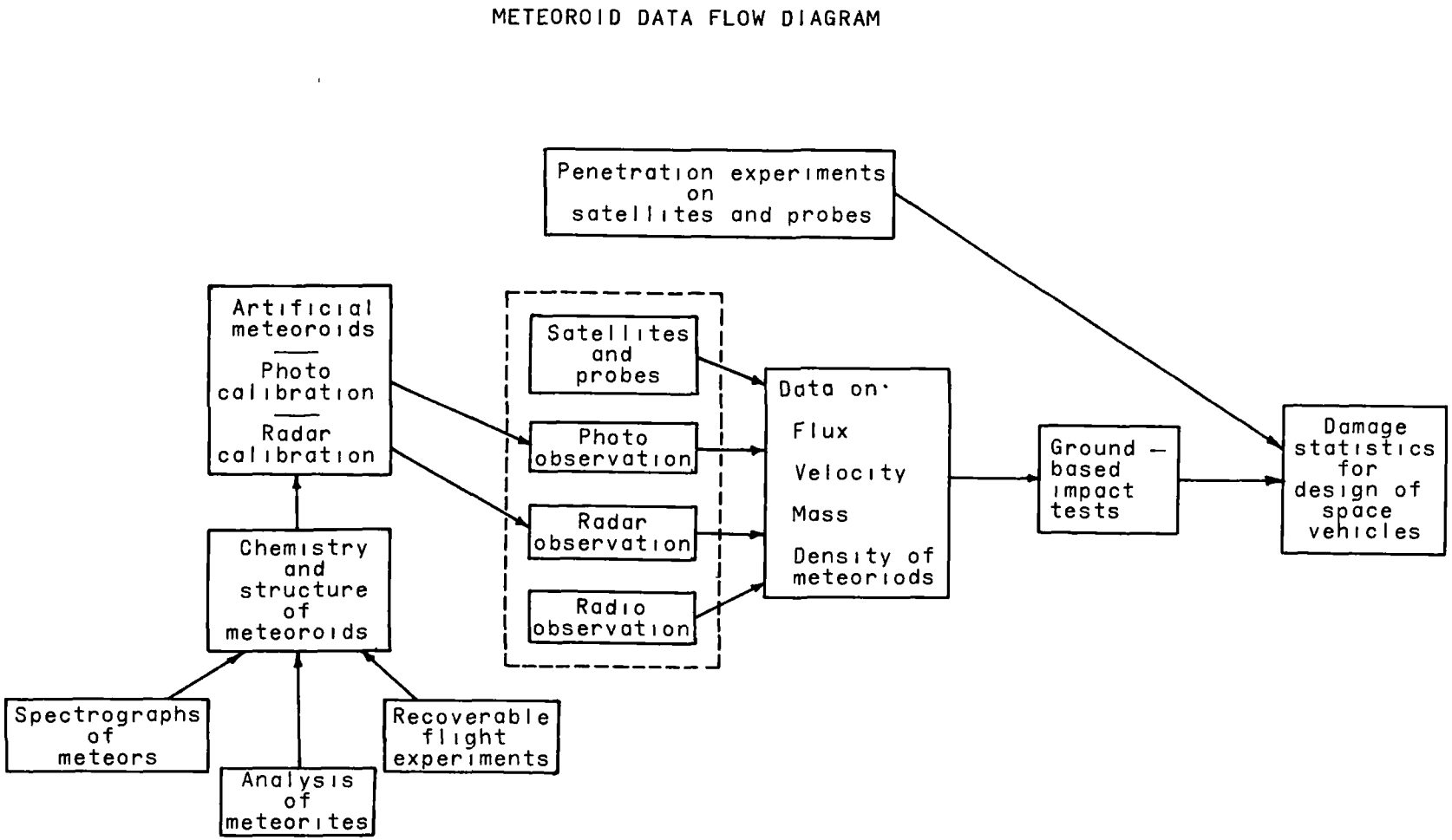

Figure 11.- Elements of meteoroid research and flow of information.